Characterization of an Interaction between *S. mansoni* surface protein NPP5 and human immune receptor LAIR-1

Edward Midgley

Master of Science (By Research)

University of York

Department of Biology

December 2024

Abstract

Schistosomiasis is an infectious tropical disease that is endemic to Africa, Asia, South America and some parts of Mediterranean Europe. This neglected disease affects over 200 million worldwide, mostly in developing countries, and is often chronic. The Schistosoma worms and larvae can regulate the immune system of their human host, allowing them to remain in the body unaffected. Research into this immunomodulation is at an early stage, and in this work, we aim to characterise an interaction between an S. mansoni protein NPP5 and a human immune receptor LAIR-1. SmNPP5 is an ectoenzyme present on the tegument of the worms and larvae. hLAIR-1 is a human receptor with immunomodulatory functions known for binding collagen: when activated via ligand binding, it will suppress the immune function of the cell it is expressed on. We used recombinant forms of both proteins and determined that the hLAIR-1 binding SmNPP5 through its Ig domain, specifically residues R59 and R65. We have also found that collagen I, the natural hLAIR-1 ligand, competes with SmNPP5 for binding to hLAIR-1. Next, we determined that SmNPP5 is likely a dimer and predicted that it homodimerizes via the residue C410.Finally, we found that the secreted paralog of hLAIR1: hLAIR2, can also bind to SmNPP5 and that this interaction can also be disrupted by collagen I.

Author Declaration

I declare that this thesis is a presentation of original work, and I am the sole author. This work has not previously been presented for a degree or other qualification at this University or elsewhere. All sources are acknowledged as references.

Abbreviations

ADP: Adenosine diphosphate; **ATP:** Adenosine triphosphate; **CDC:** Centre for Disease Control; **DNA:** Deoxyribonucleic Acid; **HBS:** HEPES-Buffered Saline; **HEK:** Human Embryonic Kidney; **hLAIR:** human Leukocyte-associated Immunoglobulin-like Receptor (1 and 2); **HRP:** Horseradish Peroxidase; **Ig:** Immunoglobulin; **ITIMs:** Immunoreceptor Tyrosine-based Inhibition Motifs; **LILRB4:** Leukocyte Immunoglobulin-like receptor subfamily B member 4; **NAD:** Nicotinamide Adenine Dinucleotide; **NICD:** NAD Induced Cell Death; **PBS:** Phosphate-Buffered Saline; **PCR:** Polymerase Chain Reaction; **RNA:** Ribonucleic Acid; **SAVEXIS:** Scalable Arrayed multi-Valent Extracellular Interaction Screen; **SDM:** Site Directed Mutagenesis; **SDS:** Sodium Dodecyl Sulphate; **SHP:** Src homology 2 domain-containing phosphatase; **SmNPP5:** *Schistosoma mansoni* Nucleotide Pyrophosphatase/ Phosphodiesterase 5; **SPR:** Surface Plasmon Resonance; **TAE:** Tris-Acetate-EDTA; **TMB:** Tetramethybenzidine; **Th:** T helper.

1 – Introduction

1.1 - Schistosomiasis

Human Schistosomiasis is a neglected tropical disease affecting more than 200 million people worldwide (1, 2). The disease is caused by parasitic worms which reside within the blood vessels of infected individuals, and is mainly endemic to Africa, but also shows presence in Asia, South America (3) and is even present in Corsica (2). There are many species of *Schistosoma* with 3 being considered the 'main' species that infect humans: *Schistosoma mansoni, haematobium and japonicum* (3). This project focuses on *Schistosoma mansoni* as it is the easiest species to maintain in a laboratory environment, and is one of the more prevalent species. It is mostly endemic to sub-Saharan Africa, but it is also found in South America. Also, the mouse model recapitulates the pathology observed in humans, providing more avenues for research.

The *Schistosoma mansoni* life cycle is shown below(Fig. 1). The eggs are released into freshwater with the faeces, where they hatch and release miracidia into the freshwater. These miracidia penetrate and infect the aquatic snail genus *Biomphalaria*, specifically *Biomphalaria glabrata* and *Biomphalaria pfeifferi* (4). These snails are an intermediate host where the miracidia develop into sporocysts and subsequently cercariae. The cercariae are released from the snails into freshwater, subsequently contaminating it. These cercariae are free-swimming larvae and can penetrate the skin of humans within the contaminated waters. These cercariae then lose their tail to develop into schistosomulae, which migrate through the blood. They first circulate to the lungs, and then the heart, before accumulating in

the hepatic portal system, where they stay until they develop into adult worms 4-5 weeks later. The adult worms then migrate to the blood vessels of the intestines, where they copulate as male and female pairs and feed on erythrocytes for energy (5). The male worm fertilizes the eggs, and the female releases them into the blood stream. Most of the eggs released from *S. mansoni* worms are excreted via faeces, however, anywhere from 30 to 50% of the eggs remain trapped within tissues (6). This happens when the eggs are backflushed by the blood supply and redirected to the liver. Trapping of eggs within the liver is the main cause of pathology for *S. mansoni* as they lodge in the sinusoids and induce granulomatous inflammation (7). Some of the eggs that are excreted via faeces end up in freshwater sources, which begins the lifecycle over again.

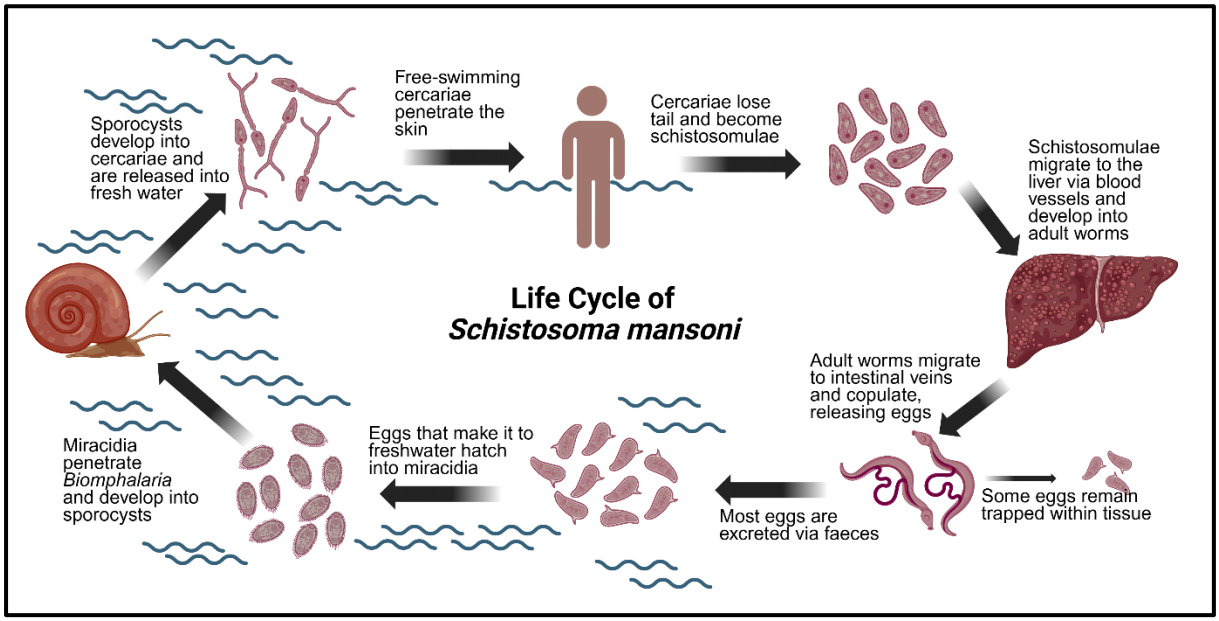

Figure 1 - ***Lifecycle of Schistosoma mansoni -*** *Eggs released by female worms may end up in freshwater, then hatch into miracidia. Miracidia penetrate aquatic snails and develop into primary and secondary sporocysts. Cercariae are then released into the water. When Humans come into contact with contaminated water, the cercariae penetrate the skin, lose their tail and become schistosomula. The parasites enter the circulatory system and migrate through the lungs and then to the liver, where they mature for 4-5 weeks into adult worms. The adult worms migrate to the mesenteric veins of the intestines and pair up as male and female copulations. The male fertilizes the eggs, and the female releases them into the bloodstream. Some eggs end up in tissues, causing inflammatory responses, however most of the eggs end up being excreted via faeces. Image created in BioRender (8).*

Each species of *Schistosoma* is specific to a different genus or species of aquatic snail, restricting the disease to areas where the snail is present. The disease is further restricted to areas and countries with poor water sanitation, as the egg-contaminated faeces must be released into freshwater without being treated at a sewage plant. Additionally, humans must also come into contact with cercariae-contaminated freshwater regularly for it to be considered endemic. Other mammalian hosts serve as reservoirs for different species of *Schistosoma*. *S. japonicum* can infect cattle, dogs, cats, rodents, pigs, horses, and goats. *S. mekongi* can also infect dogs. *S. mansoni* has been found to infect non-human primates (9) as well as rodents (10), however the CDC still considers it a human parasite and not a zoonotic disease (11).

The symptoms of Schistosomiasis mansoni are caused by the accumulation of eggs within the hepatic and intestinal tissue (12). Trapped eggs express antigens that activate an immune response targeting the eggs. The response involves an initial moderate Th1 response, shifting to a strong Th2 response. The function of the Th2 response is to protect the host from the initial inflammatory reaction. After the trapped eggs have been eliminated, the tissue remains scarred, this is the characteristic hepatic fibrosis of Schistosomiasis and is also primarily mediated by the Th2 response (7). An important distinction to make is that while the immune system can recognise and target the trapped eggs, the copulated adult worms are still releasing new eggs. This means the body is never truly free of trapped eggs, thus making Schistosomiasis a chronic condition.

The most effective treatment available for Schistosomiasis is Praziquantel and it is used widely across the world. While the precise mechanism of action is not currently known (12), we know that Praziquantel induces a Ca^{2+} influx, muscle contraction and tegument damage. We also know that a nanomolar concentration of Praziquantel can activate the transient receptor potential channel Smp_246790 (14). Praziquantel has its limitations: It can only target the adult worm stage and does not prevent reinfection later from the free-swimming larvae (3). There are also reports that the drug is less effective in areas where there is a higher rate of its use against schistosomiasis (15), and while a natural resistance to praziquantel has not yet been confirmed, resistance has been induced within a laboratory setting (16). Finally, Praziquantel requires a host antibody response to be effective (17), and is not as effective in patients that are immunocompromised.

Since Praziquantel only treats the worms, and does not prevent reinfection from cercariae, the disease ends up being chronic in nature. The schistosomula remain undetected by the immune system, and are also not known to cause schistosomiasis specific symptoms, so directly treating them after infection is not the best option. Instead, a vaccine that effectively targets the schistosomula stage, would be greatly beneficial, as it would prevent reinfection, and completely negate the chronic nature of the disease without having to diagnose the patient with schistosomiasis first.

1.2 – Finding Host-Parasite Interactions

Schistosoma have the ability to regulate and suppress immune responses to increase the worms' survival rate and have been shown to influence the immune response at many stages of the life cycle (18). The adult worms express a variety of surface ectoenzymes that can cleave host-signalling molecules, one example is SmATPDase1. SmATPDase1 is known to degrade ATP, which is a potent pro-inflammatory mediator. It also degrades the ATP derivative ADP, which activates platelets (19). The parasite eggs released by mature worms secrete proteins that modulate the human immune system, including IPSE/α1 and Omega1 (20). IPSE/α1 has been shown to dampen the inflammatory cytokine response by causing basophils to release IL-4 and IL-13. It does so by interacting with IgE bound to the FcεRI receptor on the surface of basophils. It also contains a nuclear localisation sequence, allowing it to cross the nucleus of basophils after being taken up into the cells to activate the IL-4 gene directly, however uptake into the nucleus is not required for IL-4 activation from basophils (21). Omega1 can induce a Th2 response from naïve Cd4+ T cells (22).

The investigation of the exact parasite ligands that cause this regulation is at an early stage, so this project aims to identify and characterize protein interactions between *S. mansoni* and human immune surface receptors which may cause immunoregulation. Understanding the molecular basis behind the immunomodulation caused by the larvae and worms could lead to new vaccine targets and new approaches to promote anti-worm immunity, as well as new approaches to treating undesirable immune responses in allergies and autoimmunity.

To identify host: parasite interactions, our laboratory has performed two high-throughput screens (not yet published) using the SAVEXIS technique (Fig. 2) (23).

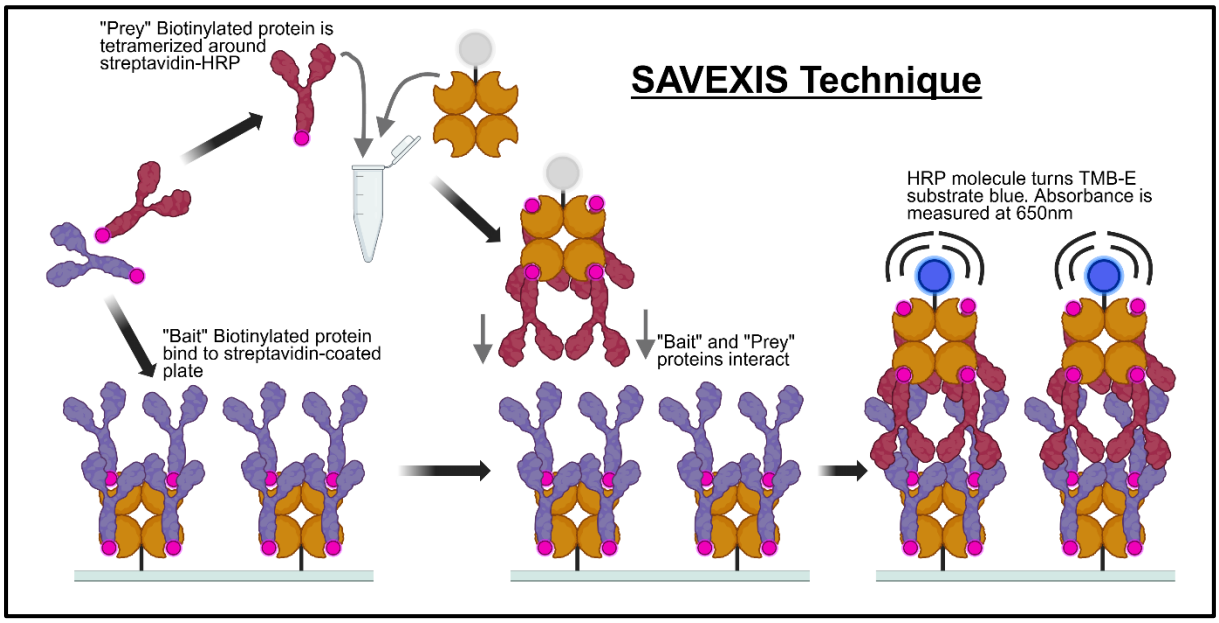

*Figure 2 - **SAVEXIS Technique** - Each human immune receptor is a "bait" protein and is bound to its own well of a streptavidin-coated plate. Each parasite protein is a tetramerized "prey" protein and is tested against the full complement of immune receptors. Image created in BioRender (7).*

In total, the screening used the ectodomains of ~400 proteins from parasites, ~120 of which were from *Schistosoma mansoni* (24) as soluble prey proteins, and tested them against a library of ~750 human surface proteins (23). Many interactions were found, but this project focuses on *S. mansoni* protein SmNPP5 and its binding to human Leukocyte receptor hLAIR-1 (Fig. 3), which is a well characterized immunomodulator (25).

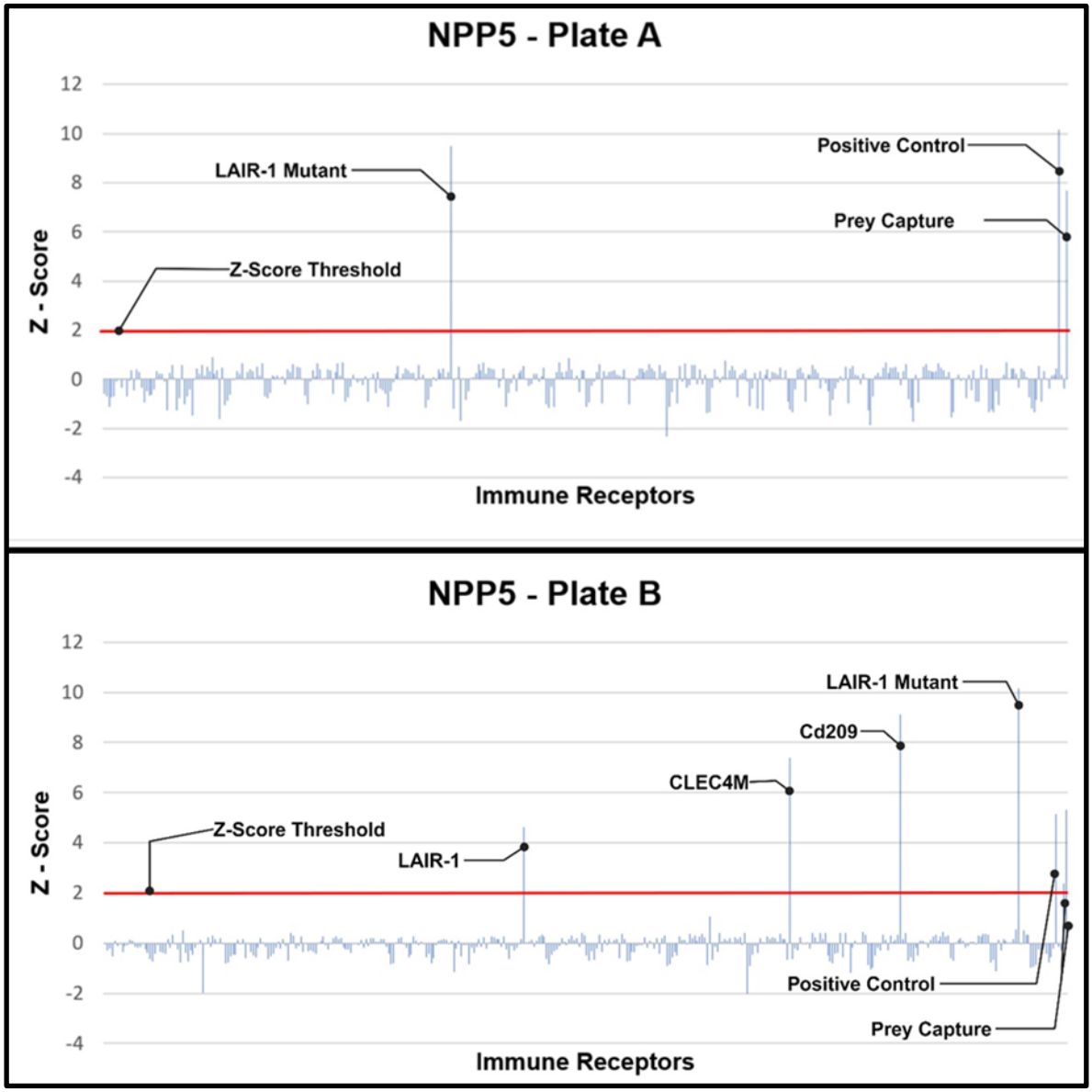

Figure 3 - ***Screening Immune Receptors for SmNPP5 Binding Partners –*** *The Z-score threshold for this screen was 2, any well where Z ≥ 2 is considered to be a positive interaction. Positive interactions were verified by repeating the experiment a total of 3 times with new stocks of proteins each time. Plate A and B are 2 halves of the leukocyte library. A) The only positive interaction with SmNPP5 here was a mutant of hLAIR1 containing a set of mutations present in public antibodies from patients with malaria. B) SmNPP5 binds multiple receptors: LAIR-1, C-type Lectin Domain member 4 family M, CD209 Antigen and the same LAIR-1 mutant again.*

While SmNPP5 did bind to mutant form of hLAIR-1 containing four point mutations, CLEC4M and CD209, it should be noted that these were very promiscuous proteins, meaning they interacted with more than 10 different pathogen proteins, and so these interactions were not progressed further. This indicates that the interactions were likely non-specific specific, or that the C-type lectins CLEC4M and CD209 interacted with glycans present on the preys.. For example, in the second screening, the hLAIR-1 mutant bound 36/72 of the *Schistosoma mansoni* proteins, CLEC4M bound 25/72 and Cd209 bound 29/72. While WT hLAIR-1 only bound 6/72. In all SAVEXIS screens, the interaction between the rat Cd200 and its cognate partner CD200R was always used as a positive control to ensure that all steps of the protocol had been followed correctly.

1.3 – hLAIR-1

hLAIR-1, or Human Leukocyte-associated Immunoglobulin-like receptor (Fig. 4A), is a type 1 glycoprotein that belongs to a large family of Inhibitory immune receptors (26). The extracellular structure contains a C2-type Immunoglobulin-like domain, and a disorganised region connecting to the transmembrane region. The cytoplasmic region contains 2 immunoreceptor Tyrosine-Based Inhibitory Motifs (ITIMs) that induce the negative control signals within the cell (Fig. 4B). hLAIR-1 requires both ITIMs to be phosphorylated by tyrosine phosphatases to induce negative signalling into the cell (27). This is triggered when the Ig extracellular domain of hLAIR-1 is bound with a ligand (26) and so the activation of hLAIR-1 on immune cells causes various immune functions to be inhibited.

hLAIR-1 can bind to different ligands such as Collagen (28, 29), complement component 1Q (C1q) (29, 30), and Surfactant Protein D(SF-D) (31). C1q and SF-D can bind to hLAIR-1 as they contain collagen-like motifs (30, 31). A recent high throughput screening (23) uncovered that hLAIR-1 can bind to itself, and further verified binding to LILRB4, another immune receptor. Not much is known about the functional consequences of the two latter interactions of hLAIR-1: hLAIR-1 and hLAIR-1: hLILRB4.

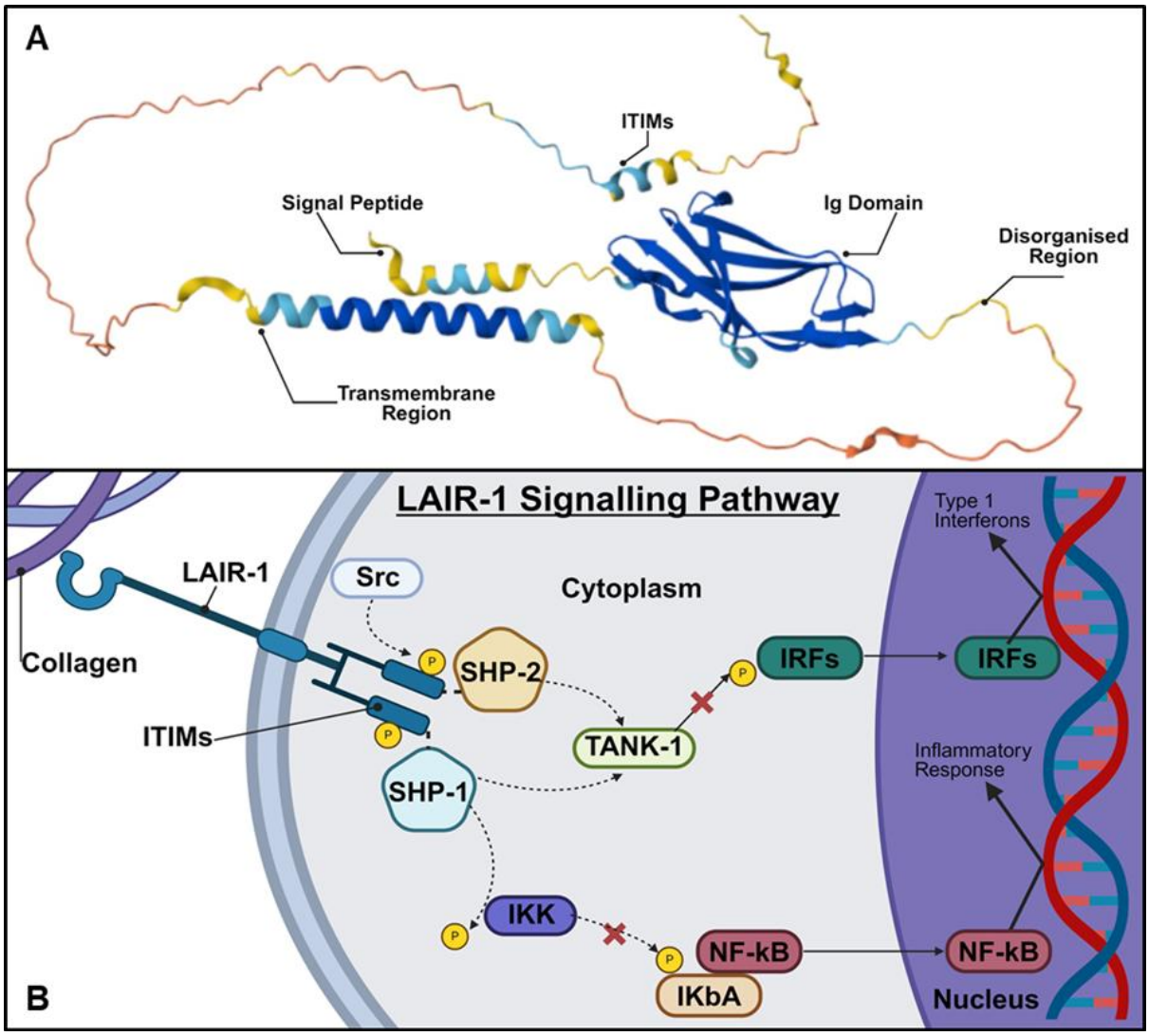

*Figure 4 - **hLAIR1 Structure and Signalling** - A) Structure is taken from AlphaFold (32, 33) and shows defined structure of hLAIR-1 full protein. The extracellular domain comprises of the signal peptide (lost upon secretion), the Immunoglobulin (Ig) domain and the disorganised region. The intracellular domain comprises of another disorganised region and the ITIMs. The disorganised regions are regions with a lack of specific secondary structure. B) hLAIR-1 is activated, Src then phosphorylates the ITIMs, which recruits SHP1 and 2, activating them. The activated SHP then activates downstream pathways (34).*

hLAIR-1 is expressed across a wide range of leukocytes including NK cells (35), T and B cells (36, 37), monocytes and dendritic cells (38). hLAIR-1 is expressed on >90% of NK cells, and their cytotoxic properties are inhibited by the crosslinking of hLAIR-1 in vitro (26). In T lymphocytes, activated hLAIR-1 inhibits T-cell receptor-mediated functions, thus inhibiting the initiation of the T-cell response (37). In naïve B cells, hLAIR-1 activation causes the diminishment of B cell activation, which has downstream effects of a decrease in IgG and IgE secretion (36). In monocytes, activation of hLAIR-1 causes the differentiation of monocytes into dendritic cells to be restricted or outright inhibited, dependent on the ligand (39). In plasmacytoid dendritic cells, expression of hLAIR-1 is the highest amongst all immune cells, and when activated, it inhibits IFNα production in response to Toll-like receptor ligands (40). We suspect that the binding of SmNPP5 to hLAIR-1 could activate some of these important pathways, so it is important to fully understand the interaction between both proteins.

1.4 – SmNPP5

SmNPP5, or Nucleotide Pyrophosphatase/ Phosphodiesterase 5, is an ectoenzyme (Fig. 5A) found on *S. mansoni* (41). Expression of SmNPP5 is upregulated during the intravascular stages of the life cycle during the schistosomulae and adult worm stages, with its highest expression being present on the male adult worms (42). It is found on the dorsal surface of the tegument, which is a double bilayer that surrounds the parasite (Figure 5B) (43).

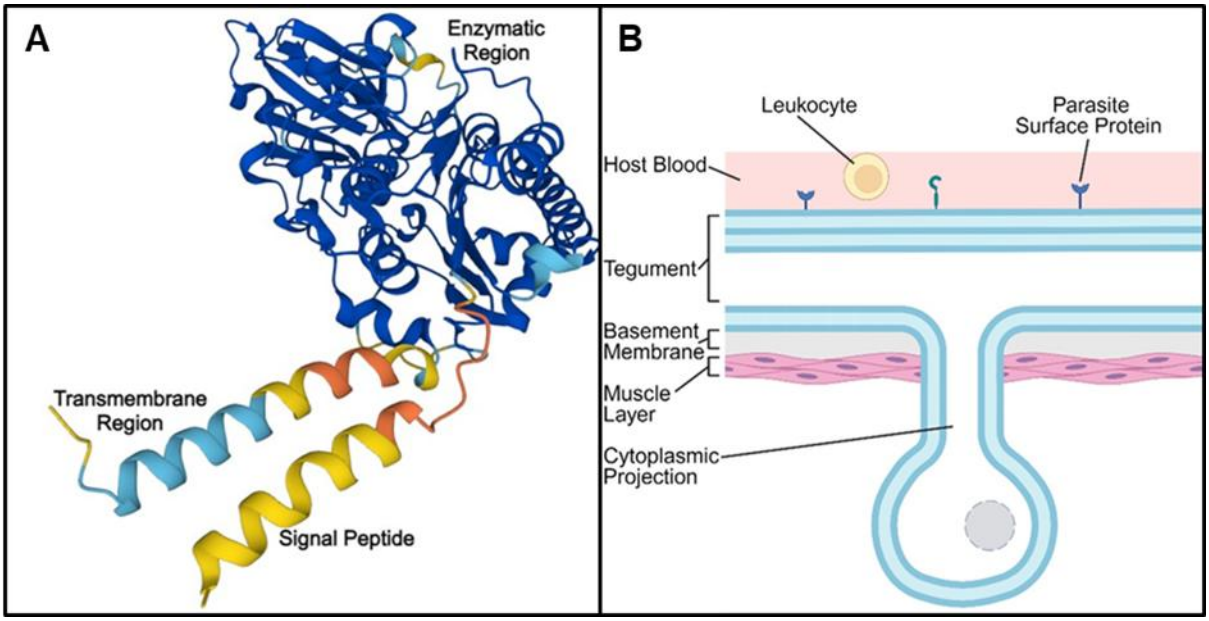

Figure 5 - ***SmNPP5 Structure and Location.*** *A) Structure is taken from AlphaFold (32, 33) and shows defined structure of the full-length SmNPP5. The extracellular domain consists of the signal peptide (cleaved from mature protein) and the ectoenzyme itself. The ectoenzyme does not have any subdomains, as it is a very globular structure. There is no intracellular domain, only a transmembrane region that anchors the enzyme to the membrane. B) Structure of the tegument and its placement upon the parasite. The tegument is a double bilayer structure that surrounds the worm. Its function is to express surface proteins that help the worm evade immune responses (44). Image created in BioRender (8).*

SmNPP5 is a major virulence factor for *Schistosoma mansoni* (42). When SmNPP5 was knocked down in the parasites using RNA interference and re-implanted into immunocompetent mice 4 days after RNAi-treatment, the number of worms recovered 28 days later was ~10 fold lower than the control group. One study suggests that may be because SmNPP5 can promote Treg survival by cleaving the signalling molecule: nicotinamide adenine dinucleotide (NAD) (45). Incubation of rSmNPP5 with NAD before adding it to a T-cell culture impeded NAD-induced cell death (NICD), presumably because rSmNPP5 had cleaved the NAD. SmNPP5 is also capable of cleaving ADP and acting as an anticoagulant by inhibiting platelet aggregation (46).

1.5 Aims and Hypothesis

The aim of our study is to investigate the molecular mechanisms underlying the tentative immune modulatory role of SmNPP5, to determine how SmNPP5 and hLAIR1 interact with each other and to investigate the functional consequences of this interaction. We hypothesise that SmNPP5 can activate the hLAIR-1 pathway, causing immunoregulation.

We also aim to investigate how this interaction compares to other known interactions involving hLAIR-1. To do this, we will:

1. Characterise the binding domains of both hLAIR-1 and SmNPP5.

2. Analyse the relationship between hLAIR-1, Collagen and SmNPP5.

3. Determine which immune cells SmNPP5 can bind to.

2 - Materials and Methods

Cloning of regions of the ectodomains

PCR fragments were amplified using KOD polymerase (Novagen) according to manufacturer's instructions for 30 cycles (Denaturing at 95°C for 20s, Annealing at 60°C for 30s, Elongation at 70°C for 60s). The reaction mixture included 50nmol of forward primer and 50nmol of reverse primer (Appendix 1), 50ng of DNA template and 25µL of 2X KOD polymerase master mix. The DNA templates corresponded to expression plasmids in which the cDNAs encoding the extracellular domain of human LAIR1 or SmNPP5 have been codon optimised for expression in mammalian cells. Template plasmids contained either the full-length ectodomain of hLAIR-1 or SmNPP5. The remaining volume was made up with ddH2O.

DNA fragments were resolved on 1% agarose gel in TAE (Appendix 1), and stained with ethidium bromide. The relevant fragments extracted using the Qiagen gel extraction kit

Restriction digests were done using restriction enzymes NotI and AscI (New England Biolabs) as the plasmids we designed had the inserts between restriction sites NotI and AscI. Both the PCR inserts and vector backbone were digested. Digests were incubated at 37°C for a minimum of 3 hours.

PCR Product Digestion Reaction Mixture: 40µL of previous PCR products, 5µL of 10x Cutsmart buffer, 0.5µL of 20U/µL NotI and 1µL of 10U/µL AscI. Volume was made up to 50 µL with ddH_2O.

Vector Plasmid Digestion Reaction Mixture: 15ug of Vector Plasmid, 5µL of 10x Cutsmart buffer, 0.5µL of NotI and 1µL of AscI. Volume was made up to 50 µL with ddH_2O.

Vector backbone digestion was subsequently run through an agarose gel to extract only the backbone and not the insert that was digested out. Digestion of the PCR inserts with NotI and AscI resulted in the production of the digested insert of interest, and of small (2-5bp) residual DNA fragments which were separated from the insert using the Qiagen PCR purification kit as per manufacturer's instructions.

The vector backbones contain a rat Cd4 d3+4 tag, for the detection or capture of recombinant proteins, a BirA biotinylation sequence, and a 6 His tag for protein purification, situated at the 3' end of the insert. If the insert does not contain a natural human signal peptide, then it is placed into a backbone that contains an exogenous human signal peptide.

To ligate the PCR insert into the digested vector backbone, each ligation solution was made up from: 60ng of digested vector backbone, 20ng of desired digested insert, 1µL of T4 DNA Ligase enzyme, 1µL of 10x Ligase buffer (Roche), and the solution was made up to 10µL using distilled water. Two controls were also performed at the same time, with almost identical reaction mixtures. The first control contained no insert and tested for single cut digestions of the vector backbone. The second control contained no insert or ligase enzyme and acted as a negative control. These reactions were left to incubate at room temperature for at least 3 hours. Ligation products were transformed in TOP10 chemically competent bacteria (Invitrogen) and the presence of the correct insert tested by colony PCR using primers 497 and 4006 (Appendix 1) flanking both sides of the insert. For each cloning, a single colony containing the correct-size insert was grown in liquid culture and plasmids were prepared using the Invitrogen Maxiprep kit according to manufacturer's instructions and sequence-verified (Eurofins) with primers 497 and 4006.

Site directed Mutagenesis PCR

Plasmids were initially amplified in two separate reaction mixtures. Mixtures contained 25µL of KOD master mix, 10ng of template plasmid, 25pmol of either forward or reverse mutagenesis primer (Appendix 1), and was made up to 50µL with ddH_2O. Both forward and reverse primers were used, but in separate mixtures. Reactions were amplified for 9 cycles (Denaturing at 94°C for 45s, Annealing at 58°C for 40s and Elongation at 72°C for 7m 30s).

Following this, the forward and reverse reactions were mixed together, adding 2μL of KOD DNA Polymerase and the same program was run again, but for 18 cycles.

Once amplified, the final PCR mixture was split into 2 halves for a DpnI digestion. DpnI is an enzyme that can only digest methylated DNA and was used to fragment the parental methylated plasmid originating from competent bacteria, however the site-directed mutagenesis (SDM) PCR products have been made by PCR and are therefore not methylated. This digestion leaves only the SDM products intact. We added 1μL of DpnI (New England Biolabs) to one half of the SDM plasmid and incubated both halves at 37°C for 3 hours. This gave us a +/- DpnI digest the SDM plasmid. We then transformed both DpnI+ and DpnI- products into chemically competent bacteria. We would expect the overall frequency of colonies from the DpnI- to be higher and this would demonstrate the digestion has been successful in the DpnI+ solution. To determine the efficiency of this protocol, we picked 10 colonies from the DpnI+ to be extracted by Qiagen miniprep kit and their insert sequenced to confirm successful mutagenesis. Of the 10 colonies picked, 8 produced usable sequences, all of which contained the expected mutation

Transfection

Biotinylated Proteins

We transfected plasmids into Human embryonic kidney (HEK) 293-6E cells, two days after passaging the cells to 500,000 cells per mL in Biotinylated Freestyle293 media (Media supplemented with 0.1% Kolliphor (Sigma-Aldrich), 0.5mg/mL G418 (Invivogen) and 0.048 mg/mL of D-biotin (Sigma-Aldrich)). For a transfection into 25mL of cells at 2,000,00 cells per ml, 2 reaction mixtures were assembled. The first was 1mL of unsupplemented freestyle media + 2.5µL of BirA plasmid at 1mg/mL + 25µL of plasmid encoding desired protein at 1mg/mL. The second was 1mL of unsupplemented freestyle media + 75µL of Polyethylenimine HCl MAX (Kyfora Bio #24765) at 1 mg/mL. These 2 mixtures were then mixed together and vortexed, then incubated at room temperature for 5 minutes before being added to the 25mL of cells. These cells were left incubating at 37°C, 180rpm, 5% CO_2 for 5 days. This was scaled accordingly for 50 and 100mL transfections

BirA is a biotin ligase that adds the biotin molecule to any protein with a BirA biotinylation sequence, such as our transfected proteins. Biotinylation cannot occur without this enzyme present.

Non-Biotinylated Proteins

This is identical to the previous protocol, except that: the media in which the transfections were prepared was Freestyle293 media still supplemented with Kolliphor, but with no D-biotin, and BirA is also excluded from the reaction mixture.

Transfection Purification

HEK293-6E cells were pelleted by centrifuging them at 800g for 25 minutes, the supernatant was then filtered through a 0.22μm sterile filter to remove any cell debris. For a 25mL transfection, 1mL of 5M NaCl and 250μL of 4M Imidazole was added to the supernatant.

For His batch purification, 25μL of Nickel-NTA beads (Thermo Fisher Scientific) were added per 25mL supernatant. This mixture was left rolling at 4°C for at least 12 hours. Following this, 5mL polypropylene columns (Thermo Fisher Scientific) were equilibrated with 5mL of 1x PBS buffer (Appendix 2) and allowed to drain by gravity. The supernatant mixture was then allowed to flow through the column, with the flow through being discarded and the nickel-beads coated with the protein of interest retained on the column. Then, 10mL of binding buffer (Appendix 2) was used and allowed to flow through to remove any contaminant proteins with a histidine-rich sequence. Finally, stoppers were added to the columns, and 250μL of elution buffer (Appendix 2) was added and left for 15 minutes. The elution buffer was then aspirated using a 1mL syringe and the eluted protein transferred to a new tube.

Protein Gel Electrophoresis – SDS-PAGE

Samples were prepared by adding 4x loading buffer (Invitrogen) and 10x sample reducing agent (Invitrogen) in a final volume of 10μL and left to denature at 80°C for 10 minutes. The Gel electrophoresis tank was set up with a NuPage 4-12% Tris Gel, which was loaded into an X-Cell Surelock Mini-Cell system (Invitrogen). Outer chamber was loaded with 1x MOPS-SDS running buffer (Invitrogen), and the inner

chamber was loaded with 200mL 1x SDS Running buffer + 500µL Antioxidant (Invitrogen). 5µL of BLUeye Protein Ladder (Jana Bioscience) and 10µL of each sample mixed with loading buffer (Invitrogen) was loaded into different wells. The gel was run at 200V and 400mA for 50 minutes, stained with InstantBlue Coomassie (Neobiotech) for a minimum of 1 hour and was observed under visible light.

Some proteins were run on a gel in non-reducing conditions, these samples were prepared using only 4x loading buffer. They were not denatured by heat or reduced by sample reducing agent.

Western Blot

Transfer buffer was prepared using 20x NuPage transfer buffer (Invitrogen), 10% methanol and 0.1% antioxidant (Invitrogen). PVDF membrane (Amersham) was activated in methanol for 30s, then rinsed in deionised water for 1 minute and finally incubated in transfer buffer for 5 minutes. The gel transfer was done overnight at 30V, 400mA in an XCell II blot module (Invitrogen).

Following transfer, the membrane was blocked using PBST/2% BSA (Appendix 1) for 2 hours. The membrane was then incubated in PBST/ 2%BSA + 0.2µg/mL Streptavidin-HRP (Pierce) for 1 hour. Membrane was then washed with PBST 3 times for 10 minutes.

To detect the HRP- conjugated streptavidin, SuperSignal West Pico chemiluminescent substrate (Thermo scientific) in a 1:1 ratio of peroxide and enhancer was dripped on the membrane. This was wrapped in cling film and the chemiluminescence was observed on an imager (Azure Biosystems c600).

Dialysis

Some proteins were dialysed using 'Millipore^{TM} D-Tube Midi Dialyzer'. Protein solution was transferred to these D-Tubes and the tubes were placed into a foam block so they could float in the correct orientation. This was spun in buffer for 2 hours. The used buffer was then replaced with fresh HBS (Appendix 2), and the process was repeated twice, with the final buffer exchange taking place overnight' The dialyzed proteins solution was then recovered.

Bradford Assay

Serial dilutions of Albumin standard were made to create a standard curve, the top concentration was 1200ng/µL and was diluted 5/3 in elution buffer. For both standards and purified proteins of interest, 10µL proteins were mixed with 150µL of Bradford assay reagent (Thermo Fisher Scientific). The plate was left shaking for 30 minutes until it was observed at an absorbance of 595nm on a plate reader (TECAN SPARKS).

SAVEXIS

The SAVEXIS assay is a method of detection of protein-protein interactions and can be done for proteins with very low affinities for each other. The proteins must be biotinylated. It works by having the 'Bait' proteins immobilised to a streptavidin coated plate via the biotin, then a 'Prey' protein is incubated with the "bait". The 'Prey' is composed of 4 identical proteins tetramerized around a single Streptavidin-HRP molecule via the biotin.

100µL of ‘Bait’ proteins were arrayed in individual wells of a streptavidin coated microtitre plate at a concentration of 4.5nM. The plate was the incubated at 20°C for 1 hour. During this incubation, prey proteins were tetramerised by mixing the biotinylated protein of interest at 17.5nM to streptavidin-HRP at 10nM in a 2.5:1 volume ratio, respectively. After a 60 minute incubation, the now tetramerized ‘Prey’ proteins were diluted 20-fold in HBS/2%BSA to bring them to 0.625nM. Following the incubation of the ‘Bait’ proteins, the contents were removed, and then subsequently washed 3 times with 150µL of HBS-T/desthiobiotin (Appendix 2) to block the unoccupied streptavidin sites in the well. Preys were then arrayed into the appropriate wells at 100µL per well. The plate was in then incubated at 20°C for 1 hour. The contents were then removed and the plate was washed with 150µL of HBS-T/desthiobiotin per well twice and then 150µL of just HBS per well for the final wash. 100µL of TMB-E(Millipore) substrate were then added to all wells used and incubated at 20°C for 30 minutes. The reaction was then stopped by adding 100µL of 0.3% NaF. The absorbance was measured at 650nM on a plate reader.

SAVEXIS – Non-biotinylated Bait Proteins Variation

Non-biotinylated proteins will not bind to the streptavidin coated plate as they do not have a biotin group. Instead, they must be adsorbed to a Maxisorp plate. To do this, they were diluted in buffer (0.1M Na_2HPO_4 ,9.0 pH) to 5nM, 100µL was then arrayed to all necessary wells and left to adsorb to the plate at 4°C overnight. The preys were then tetramerized to streptavidin-HRP (as described in above) and left to incubate for 1 hour. After the unbiotinylated proteins had been absorbed, the plate was flicked out and washed with 150µL of HBS-T 3 times, flicking out the liquid each time. After the

tetramerization of the preys, they were diluted 20-fold and 100µL was arrayed to their respective wells and left to incubate for 1-2 hours. This was washed out using 150µL HBS-T twice and then HBS once. 100µL of TMB-E was then arrayed to all wells used and left to incubate for 30 minutes before measuring the absorption at 650nm.

SAVEXIS – Competition Variation

For this experiment, we prepared the bait and arrayed it on a streptavidin coated plate. The prey was tetramerized around streptavidin-HRP as described above. When diluting the tetramer to its final working volume, a non-biotinylated competitor was added into the dilution in an attempt to interfere with the binding of the prey. The competitor is usually a protein that has the potential to compete with the prey for binding to the bait. The Bait protein was removed and the plate was washed with HBS/T desthiobiotin 3 times. The prey + competitor mixture was incubated for 30 minutes at room temperature, then arrayed to the appropriate wells on the streptavidin coated plate. This plate was incubated for 1 hour before the contents were flicked out. The plate was then washed out with HBS/T desthiobiotin 2 times and HBS once, for the final wash. 100 µL of TMB-E(Millipore) substrate was then added to all wells used and incubated at 20°C for 30 minutes. The absorbance was measured at 650nM.

Surface Plasmon Resonance

Experiments were performed on a Biacore T200 using a Cytiva Biotin CAPture Chip in SPR Buffer (Appendix 2). The purified analyte protein was non-biotinylated, and was gel filtrated on a Superdex 200 column using an AKTA Pure instrument immediately before the experiment.

This experiment was designed to compare analyte binding between a control flow cell coated with the negative control Cd4 tag (Fc1) and an experimental flow cell coated with the Cd4-tagged protein of interest (Fc2).

First, we prepared the CAP chip with biotin capture reagent on both Fc1 and 2 until it was relatively equal on both flow cells at ~3500 Response units (RUs). We then proceeded to capture both Cd4 and SmNPP5 on Fc1 and Fc2 respectively, in this case, the RUs added is directly proportional to the molecular weight of the proteins; so, we have to account for the 3.14:1 ratio between the molecular weights of SmNPP5 (89 kDa) and Cd4 (28 kDa), respectively. In total, ~580 RU's of Cd4 were added to Fc1, and ~1850 RUs of SmNPP5 were added to Fc2. Binding measurements were performed by injecting the analyte at 10 µl/min for 60 seconds.

3 – Results

hLAIR1 interacts with SmNPP5 through its Ig domain

Using the SAVEXIS assay, we had previously probed SmNPP5 against a collection of 750 human receptors and identified hLAIR1 as a tentative binding partner. In this initial assay, all human receptors “baits” had been arrayed on streptavidin-coated microtitre plates and an HRP-tagged tetrameric SmNPP5 “prey” used to identify binding partners. To validate this initial observation, we produced new protein preparations (Fig. 6A) to demonstrate that this interaction could be replicated. We also demonstrated by SAVEXIS that the interaction was independent of the bait: prey orientation (Fig. 6B).

Our next goal was to identify the domain of hLAIR-1 responsible for this interaction. The extracellular domain of hLAIR1 is composed of an N-terminal immunoglobulin (Ig) domain followed by a C-terminal disorganised region. We used PCR and restriction digestions to subclone each subdomain into its appropriate expression vector. Following ligation and sequence confirmation, plasmids were transfected into HEK293-6E cells for recombinant protein expression and subsequent purification (Fig. 6A), before using SAVEXIS to determine the hLAIR-1 binding domain (Fig. 6C & D).

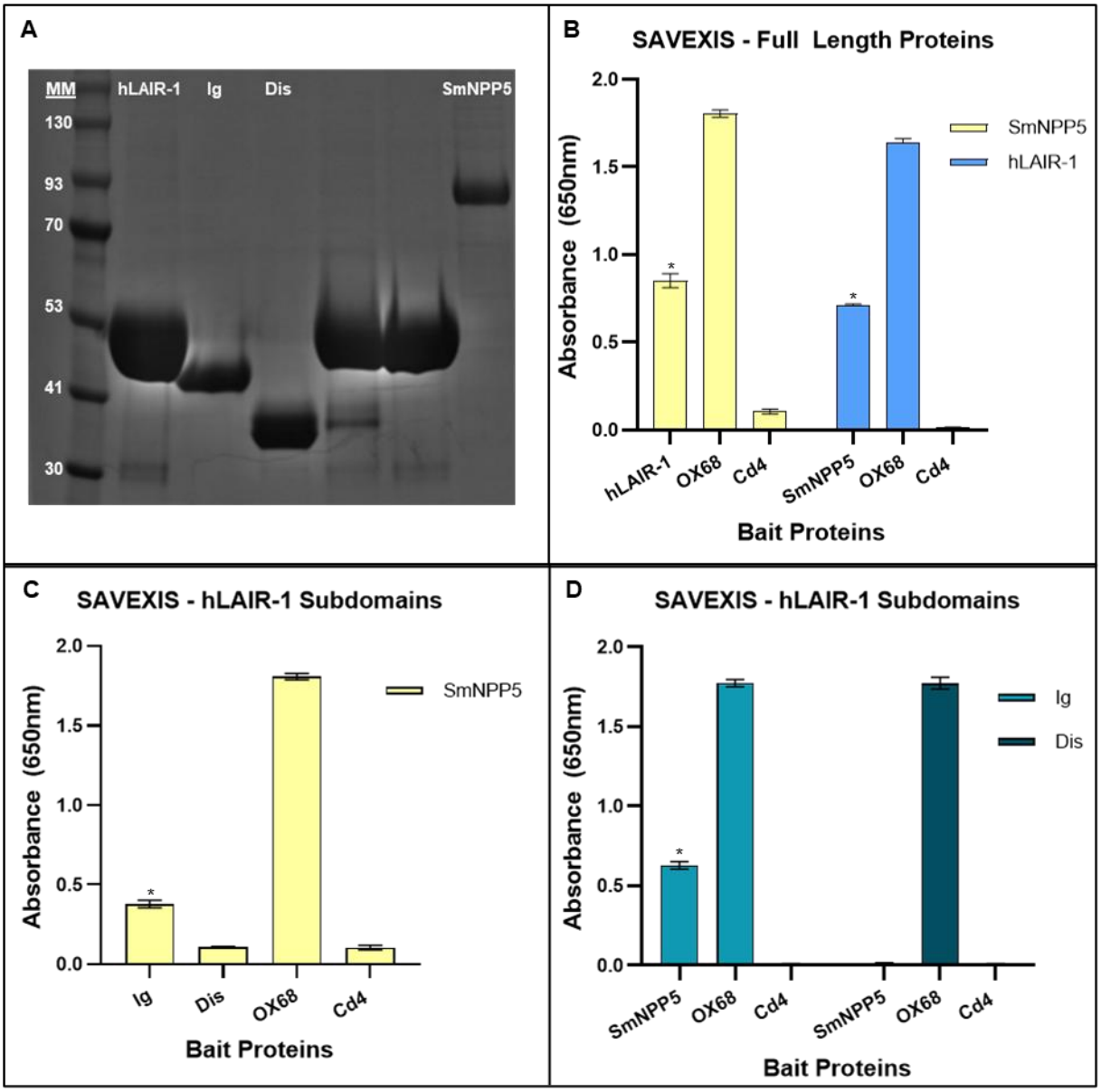

*Figure 6 - **hLAIR-1 binds to SmNPP5 through its Ig Domain** –A) An SDS-PAGE protein gel showing recombinant hLAIR-1 full length, Ig and disorganised domains and SmNPP5. MM: molecular masses marker. B-D) SAVEXIS determination of binding of B) full length ectodomains of hLAIR-1 and SmNPP5 to each other in both orientations. Left (yellow) show SmNPP5 as prey binding to indicated baits. Right (blue) shows hLAIR1 as prey binding to baits. C) hLAIR Ig domain and disorganised subdomain baits to SmNPP5 prey, and D) SmNPP5 bait to hLAIR Ig domain (light blue) and disorganised subdomain (dark blue) preys. OX68 is an antibody used as a positive control bait that specifically binds the Cd4 tag present on each recombinant prey. Cd4 is a negative control bait that should not bind any prey, so revealing extent of non-specific background for each prey. Experiment repeated technically n=5, error bars represent mean -/+ standard deviation. Statistical significance determined by unpaired t- test compared to Cd4 negative control (* represents p<0.0005).*

Binding to SmNPP5 could only be detected with the Ig domain of hLAIR1 irrespective of its use as a bait (Fig. 6C) or as a prey (Fig. 6D). No binding could be detected with the disorganised region of hLAIR1. We therefore conclude that binding to SmNPP5 is achieved through the Ig domain of hLAIR1.

Recombinant LAIR1 proteins have expected biochemical properties

We next aimed to demonstrate that our recombinant hLAIR1 proteins produced in mammalian cells had retained the same function as their natural counterparts. In a first set of experiments, we tested binding of an anti-hLAIR-1 antibody (clone DX26). We used serial dilutions of the antibody to demonstrate that the antibody could bind the recombinant full length ectodomain in a dose-dependent manner. In addition, we could demonstrate that the binding epitope was restricted to the Ig domain of hLAIR1 since no binding was observed with the disorganised region (Fig. 7A).

Since hLAIR-1 is a known collagen receptor, we decided to use this property as a secondary verification. Using native human collagen I immobilised on a microtitre plate, we could demonstrate that our recombinant hLAIR-1 was able to bind its main binding partner, and that this binding was solely mediated by the Ig domain with no detectable binding of the disorganised region (Fig. 7B).

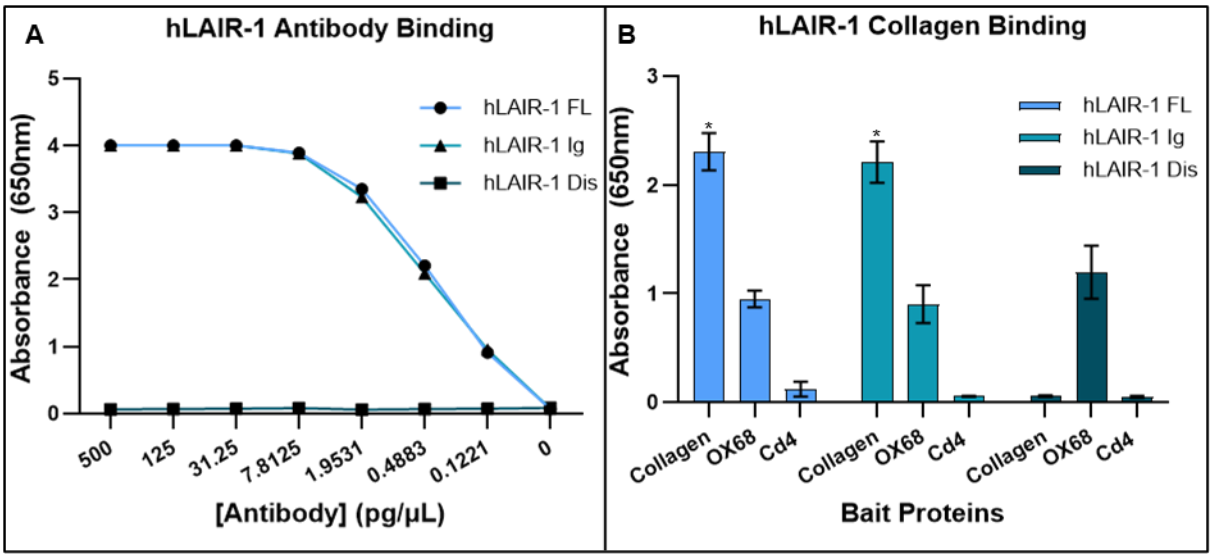

Figure 7 - ***Collagen I and Antibody can bind hLAIR-1 Full ectodomain and Ig subdomain****– A) An anti-hLAIR-1 antibody can bind the recombinant full-length and Ig domain of hLAIR-1. 450 pmol full-length, Ig or disorganised LAIR1 were immobilised on a microtitre plate and incubated with serial dilutions of an anti-hLAIR1 antibody. B) The recombinant full-length and Ig domain of hLAIR-1 can bind human collagen I. Human collagen was immobilised on a microtitre plate and incubated with HRP-tagged tetramers composed of either full-length hLAIR1, its Ig domain or its disorganised region. OX68 bait is used as a positive control to capture each prey through the Cd4 tag present at the C-terminus of each protein. Cd4 bait is a negative control to show any background noise the prey may produce. N=4. Error bars show +/- 1 standard deviation. Unpaired T-test values compare the interaction to the Cd4 negative control for that prey, showing if they are statistically different. (* represents p<0.0005).*

Prediction of SmNPP5 binding domain by AlphaFold modelling

To determine the binding domain of SmNPP5, we first used AlphaFold 2 (32, 33) to computationally predict the binding structure between the extracellular domains of hLAIR-1 and SmNPP5. The highest confidence prediction is shown below (Fig. 8). The pLDDT score is the algorithm's confidence in the structure it has presented, it is on a scale of 0-100. A score less than 50 is considered low confidence, and a score higher than 90 is considered very confident. The pTM score is a measure of how accurately the algorithm has predicted the structure of the complex, this is on a scale of 0-1, with 1 being the most accurate. This prediction suggested that a tentative binding domain would be located between residues N98 and R121 of SmNPP5. We

first designed primers to test whether we could express two separate fragments of the enzyme. We decided to cleave the protein between S253 and S254.

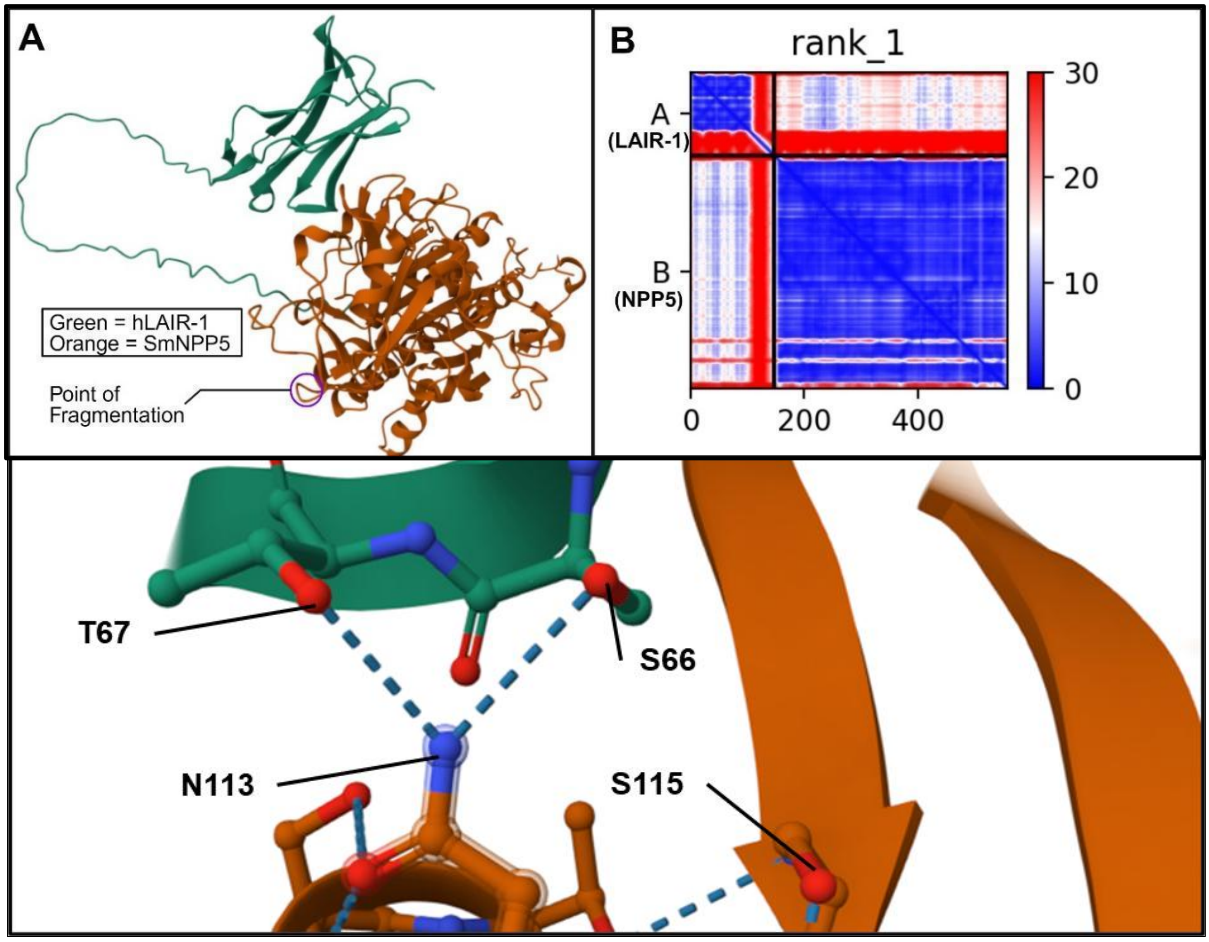

Figure 8 - ***AlphaFold Prediction of binding between SmNPP5 and hLAIR-1*** *– A) The highest confidence predicted crystal structure of the protein complex. pLDDT score is 83.3, pMT score is 0.729, ipMT score is 0.171. B) PAE confidence chart for the crystal structure shown in panel A. A lower score (blue) is higher confidence. C) SmNPP5 N113 predicted interactions with hLAIR-1. Figure shows how N113 residue on SmNPP5 hydrogen bonding to different residues. Green is hLAIR-1, Orange is SmNPP5. Predictions were made with AlphaFold 2 (32, 33).*

Expression of these SmNPP5 subdomains was unsuccessful as the truncation likely caused misfolding of the protein. We therefore decided to use the best AlphaFold prediction to compile a list of the predicted binding residues on SmNPP5 that appear involved in the binding to hLAIR-1 (Table 1).

SmNPP5	hLAIR-1
N98	I166
I104	W109
I105	R59
N106	R59
T108	R65
S111	I166
R112	E162
R112	L164
N113	T67
N113	S66
D119	Y68
R121	D70

*Table 1 - **The Predicted Binding Residues for SmNPP5 and hLAIR-1**. Residues in the same row are predicted to interact with each other, mostly through hydrogen bonds. Predictions shown here are from the highest confidence prediction shown in Figure 8.*

We chose 2 residues from this list for site-directed mutagenesis: N113 as it is predicted to have 2 binding partners, and T108 as it is predicted to bind a known collagen-binding residue on hLAIR1. Using site-directed mutagenesis, these residues were mutated to give T108A and N113A and confirmed by sequencing. However, after transfection, the N113A mutant did not express, whereas the T108A mutant did. We used it in a SAVEXIS against the full length ectodomain of hLAIR-1 to determine if the T108 residue of SmNPP5 is involved in the interaction with hLAIR1.

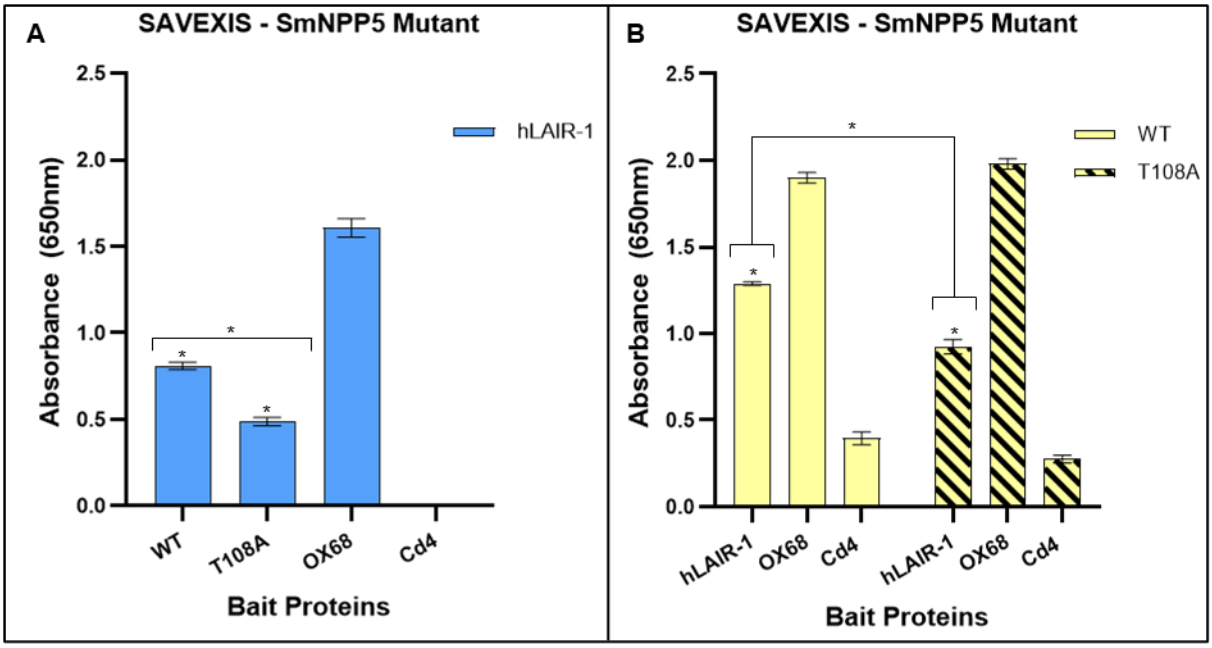

*Figure 9 - **The T108 residue of SmNPP5 contributes to the interaction with hLAIR-1** - SAVEXIS determination of binding of A) hLAIR-1 prey tested against WT and T108A mutant SmNPP5 baits. B) WT and T108A mutant preys interacting with the hLAIR-1 bait. OX68 is an antibody used as a positive control bait that specifically binds the Cd4 tag present on each recombinant protein. Cd4 bait is a negative control that should not bind any prey, so revealing extent of non-specific signal from each prey. Experiment repeated technically n=5, error bars represent mean -/+ standard deviation. Statistical significance determined by unpaired t-test. WT and T108A were compared to each other (Enclosed in Brackets) and they were also compared to the Cd4 negative control (Not in brackets). (* represents p<0.0005).*

The T108A “bait” protein showed a fainter binding signal to hLAIR1 prey compared to its wildtype counterpart (Fig. 9A). This was also observed in the reverse orientation, when SmNPP5 was used as a prey. Here again, a fainter binding signal was observed for T108A despite both wild type and mutant preys showing similar activity as shown by capture by the OX68 positive control. These observations suggest that, although mutation of T108 is not sufficient to fully abrogate SmNPP5 binding to hLAIR1, it may contribute to the interaction.

SmNPP5 behaves like a dimer

In mammals, certain members of the ENPP family are known to dimerise, such as ENPP1 (47). Guided by this information we decided to test if SmNPP5 was likely to do the same. We first used size exclusion chromatography to determine the elution profile of our recombinant SmNPP5 and compared it to the elution profiles of 2 molecular marker proteins: aldolase (158 kDa) and conalbumin (75 kDa) to that of our recombinant SmNPP5 (Fig. 10A). SmNPP5 eluted at a higher molecular weight than aldolase, suggesting that SmNPP5 is likely a ~180kDa dimer.

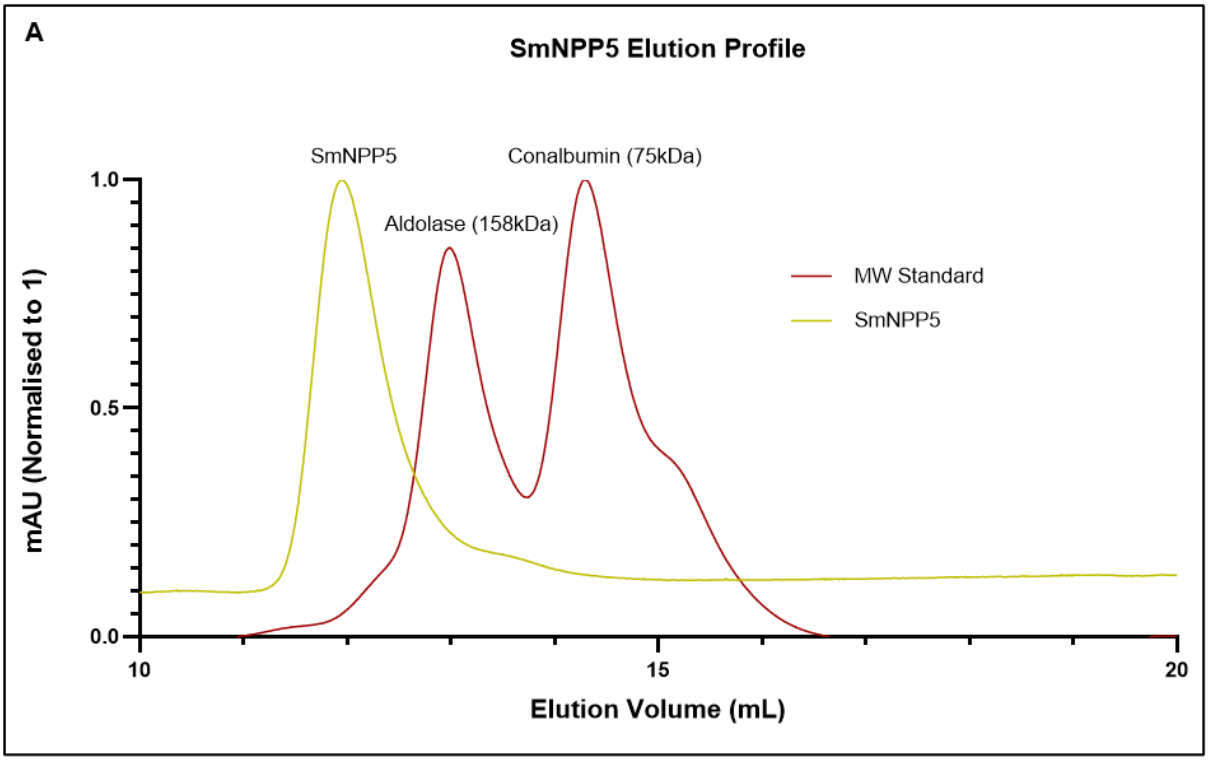

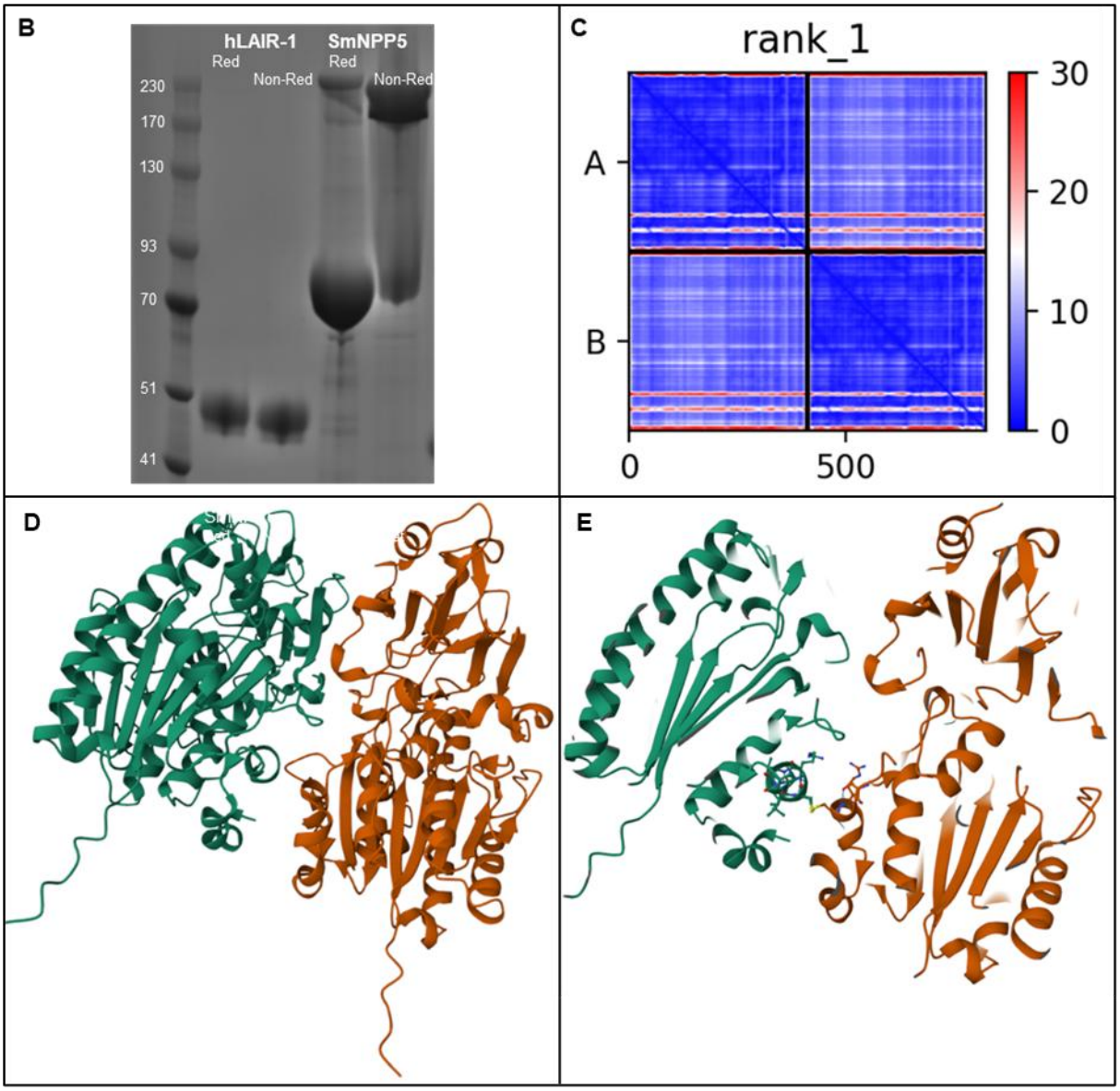

Figure 10 - ***SmNPP5 behaves like a dimer*** *– A) Gel elution profile of SmNPP5 (yellow) and molecular weight standards (red) after migration on a Superdex 200 column. Y axis has been normalised to 1. B) Protein gel comparing the reduced (Red) and non-reduced (Non-red) forms of SmNPP5 and hLAIR-1. In the reduced samples, sample reducing agent was added to reduce the disulfide bonds. Numbers represent molecular masses in kDa. hLAIR1 behaved like a monomer in both reducing and non-reducing conditions, while SmNPP5 mostly behaves like a dimer in non-reducing conditions. C) PAE confidence chart for the crystal structure shown in panel D and E. A lower score (blue) indicates higher confidence, and a higher score (red) is lower confidence. Predictions were made with AlphaFold 2. D) Highest confidence predicted crystal structure of the interaction between 2 SmNPP5. pLDDT score is 91.7, pMT score is 0.87, ipMT score is 0.806. E) The same prediction as shown in panel D highlighting the covalent bond joining both SmNPP5 proteins through C410. Predictions done by AlphaFold (32, 33).*

To confirm these observations, we then resolved the purified protein by SDS-PAGE in denaturing and non-denaturing conditions (Fig. 10B): while SmNPP5 mostly appeared as a monomeric form at ~89kDa in reducing conditions, it was mostly observed as a dimeric form at ~180 kDa in non-reducing conditions.

Finally, we used Alphafold multimer to investigate *in silico* prediction of dimerization. SmNPP5 was predicted to form a homodimer (Fig. 10C and D), with both proteins likely to be in the same cis orientation. Dimerization is likely to occur through a disulphide bridge between C410 on both SmNPP5 proteins (Fig. 10E).

Collagen and SmNPP5 Compete for binding of hLAIR-1

Having demonstrated that the anti-LAIR1 antibody DX26 is able to bind the Ig domain of hLAIR1 (Fig. 7A), we then tested whether it was able to block hLAIR1 from interacting with SmNPP5 (Fig. 11A). hLAIR1 was immobilised as a bait on a microtitre plate and incubated with mixtures containing a fixed concentration of SmNPP5 prey and a dilution range of DX26 antibody. Binding of the SmNPP5 prey to hLAIR1 was measured by absorbance at 650nm. At higher concentrations, the DX26 antibody was able to block binding of the SmNPP5 prey in a dose-dependent manner.

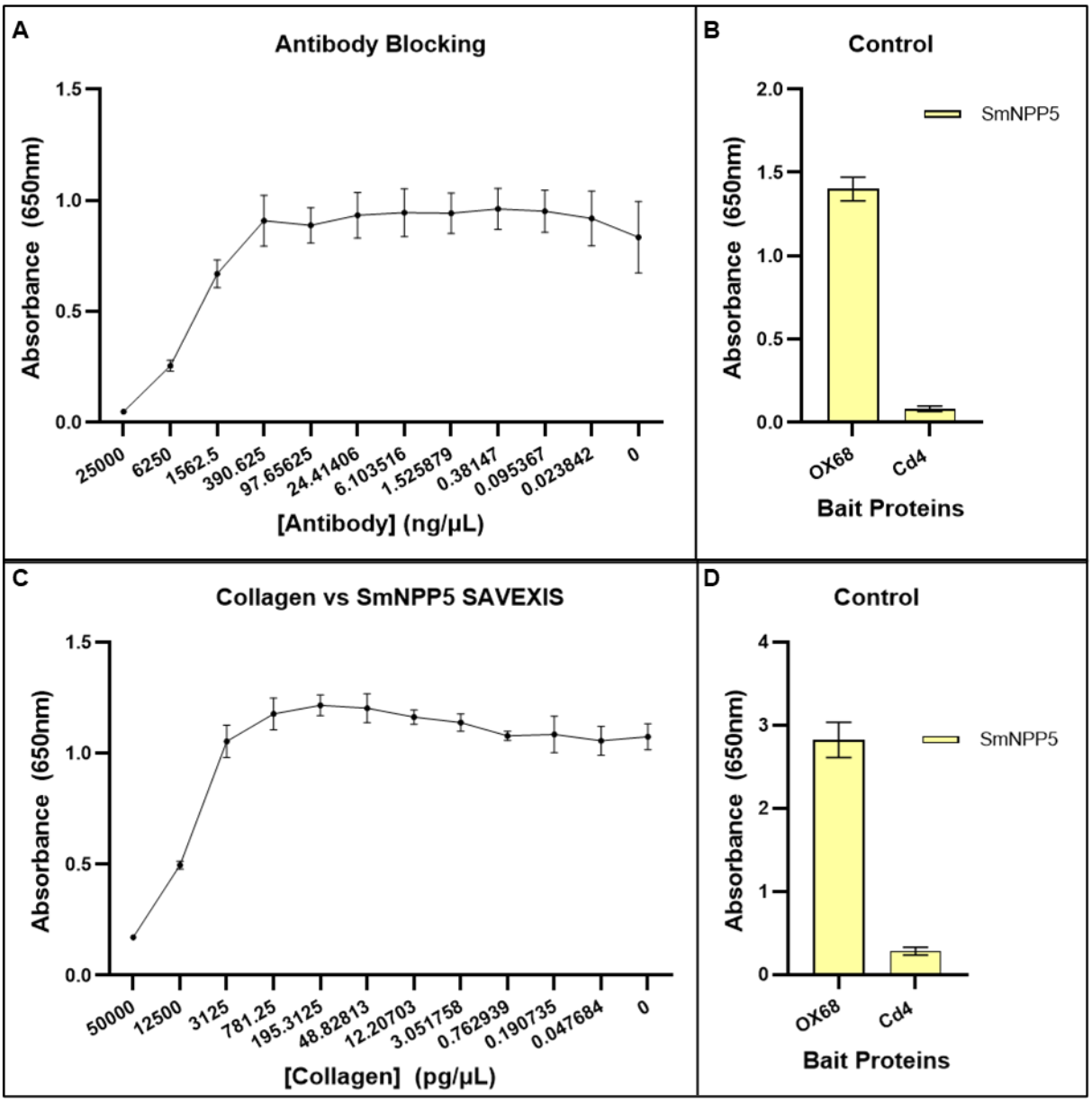

*Figure 11 - **The DX26 antibody and Collagen I block binding of SmNPP5 to hLAIR-1** – A) Competition SAVEXIS using a dilution range of anti-hLAIR-1 DX26 antibody to block binding of the SmNPP5 prey to hLAIR1 in a dose-dependent manner. B) Controls for panel A showing capture of the SmNPP5 prey by the OX68 antibody (positive control) and background signal of the prey against the CD4 negative control. C) Competition SAVEXIS using a dilution range of human collagen I to compete against SmNPP5 for binding to hLAIR-1. D) Controls for panel C as explained in panel B. Experiment repeated n=3, error bars represent mean -/+ standard deviation.*

Because collagen I is one of the main known endogenous binding partners for LAIR1, we then tested whether SmNPP5 and collagen were able to compete for binding to hLAIR1 (Fig. 11C). Figure 6C shows that collagen I can also block the binding of tetramerized SmNPP5 to hLAIR-1 in a dose-dependent pattern. Relatively

higher concentrations of collagen I block the interaction completely, whereas relatively lower concentrations don't block the interaction at all. Figures 11B and 11D shows that the SmNPP5 prey is sufficiently tetramerized as the OX68 capture was successful, while the Cd4 negative control demonstrates low background noise. We then decided to test whether mutations of two hLAIR1 residues known to be involved in collagen binding could also abolish binding to SmNPP5 (47). We chose R59 and R65 as they were both previously predicted to bind SmNPP5 (Table 1) and mutated them both to Alanine making R59A and R65A point mutations. We tested their binding to SmNPP5 in a SAVEXIS assay.

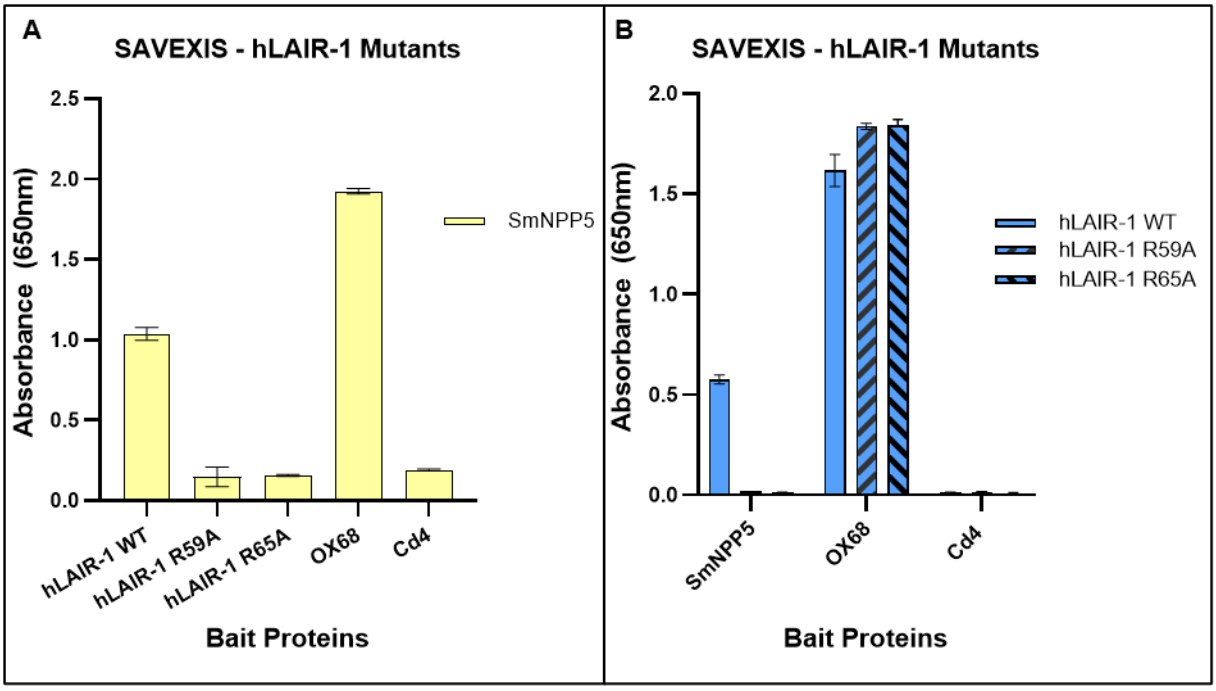

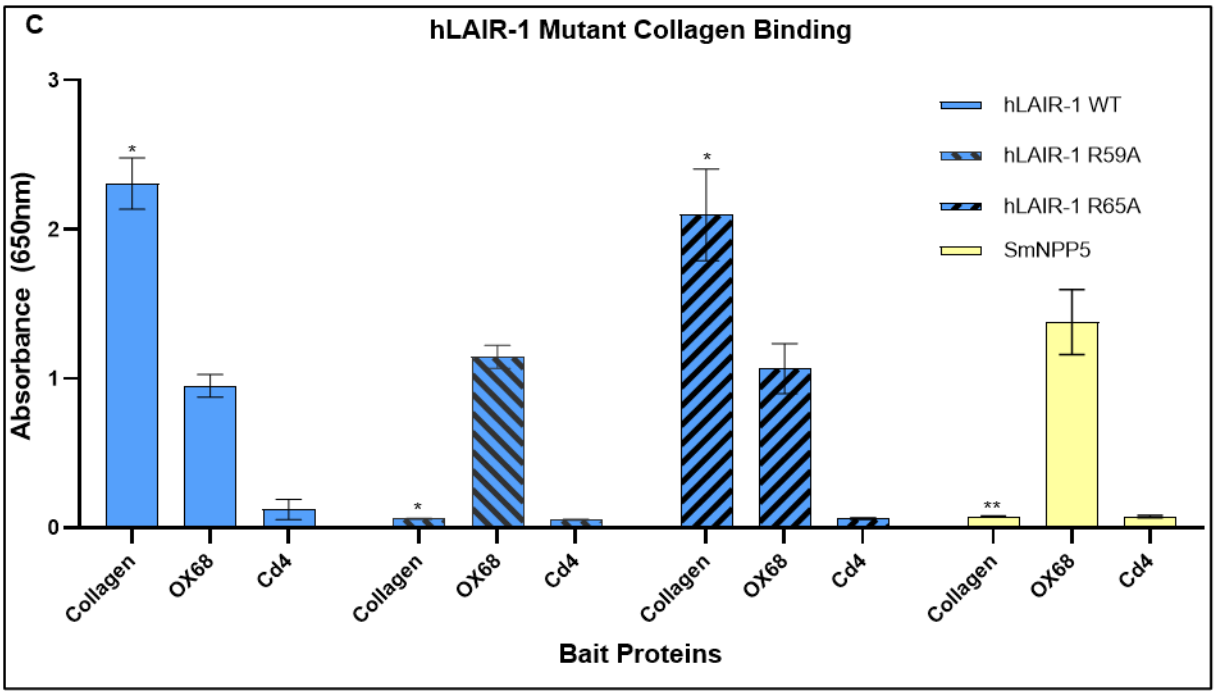

*Figure 12 - **R59 and R65 are hLAIR-1 binding residues to SmNPP5** -SAVEXIS determination of binding of A) SmNPP5 prey tested against R59A and R65A baits. B) R59A and R65A prey interacting with the SmNPP5 bait. C) hLAIR-1 + mutants R59A and R65A, and SmNPP5 prey binding to human collagen I. The legends represent the different prey proteins used. OX68 is an antibody used as a positive control bait that specifically binds the Cd4 tag present on each recombinant protein. Cd4 is a negative control bait that should not bind prey, so revealing extent of non-specific interactions. Error bars represent mean -/+ standard deviation. Statistical significance determined by unpaired t-test compared to Cd4 negative control. Panels A and B, n=5. Panel C, n=4. All repeats were technical repeats using the same batch of proteins. (* represents p<0.005, ** p=0.52).*

SmNPP5 prey could not bind to either of the hLAIR-1 mutants R59A and R65A, whether the mutants were used as baits (Fig. 12A) or preys (Fig. 12B).

We also tested the ability of the hLAIR-1 mutants and of SmNPP5 to bind collagen I. Figure 12C shows that neither the recombinant hLAIR-1 mutant R59A nor the SmNPP5 preys could bind the collagen I bait. However, the R65A mutant prey retained the ability to bind collagen I. Therefore, R59 and R65 are likely to be involved in the binding of hLAIR1 to SmNPP5. However, these binding residues do not behave in exactly the same way regarding binding to human collagen I.

hLAIR-1: SmNPP5 Interaction was undetectable by SPR

With the initial interaction repeated and verified by SAVEXIS, we wanted to determine the affinity of this interaction. To do this, we used surface plasmon resonance (SPR). We immobilised the rat Cd4(d3+4) as a negative control in the reference flow cell (Fc1) and a molar equivalent of SmNPP5 in the ligand flow cell (Fc2). Following this setup, we started to inject the analyte: unbiotinylated hLAIR-1. Surface plasmon resonance works by comparing binding of a given analyte to the reference and experimental flow cells, the expectation being that the analyte will preferentially bind to the proteins displayed in the ligand flow cell (SmNPP5) compared to the reference flow cell (Cd4). However, during this preliminary experiment, we were unable to detect any interaction via SPR (Fig. 13).

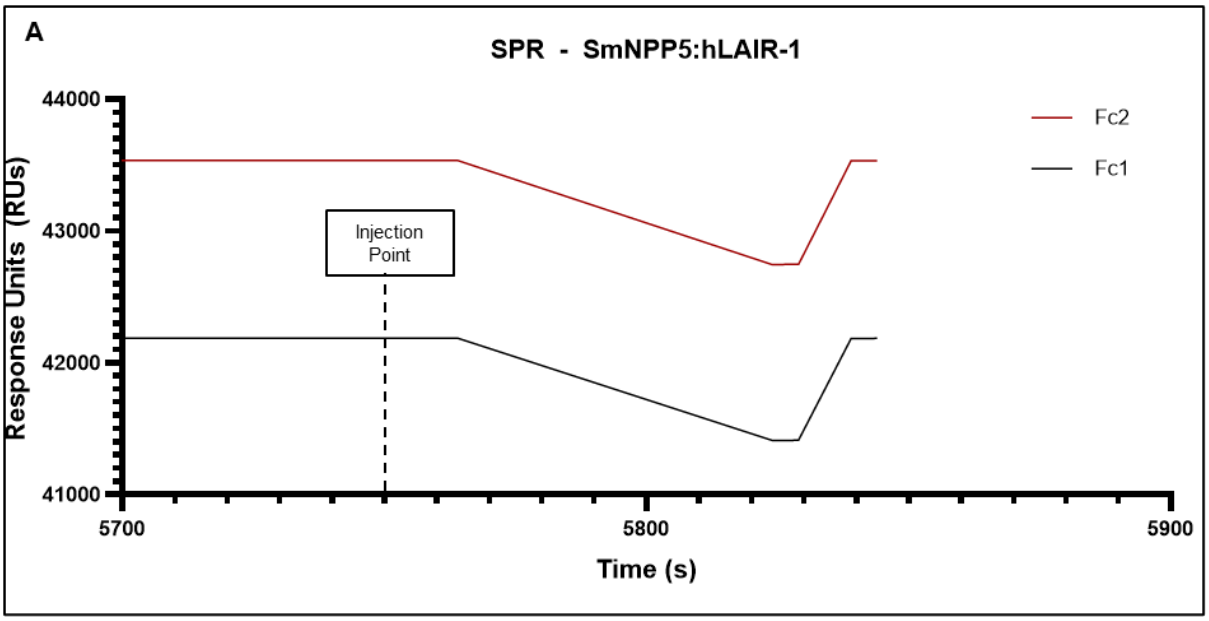

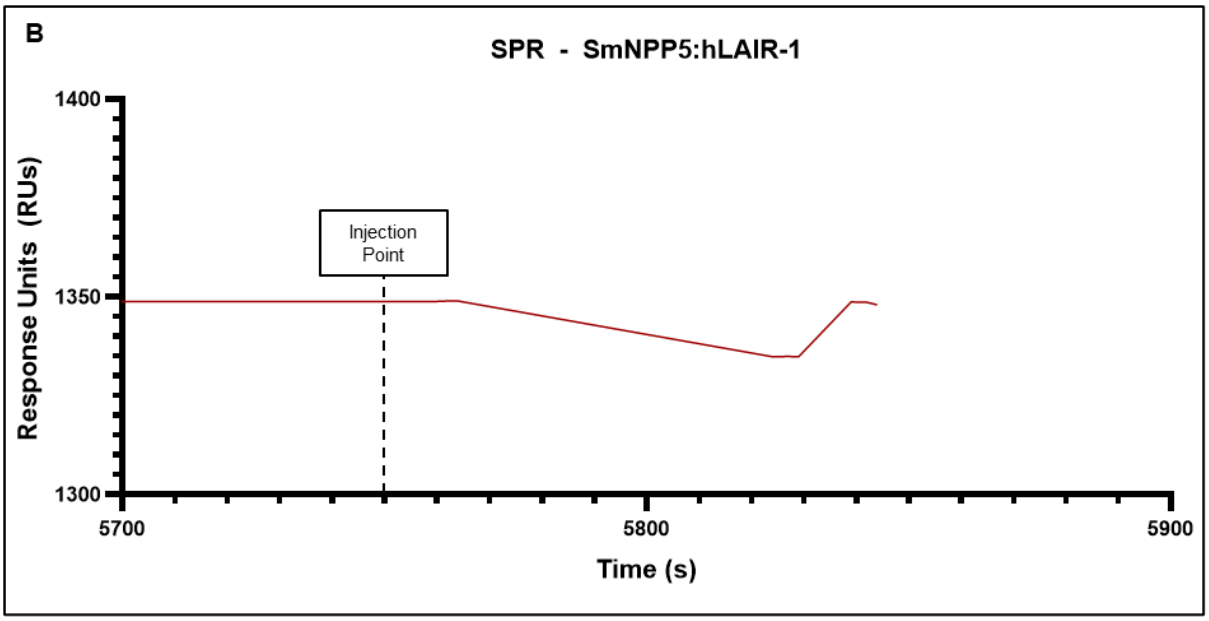

*Figure 13 - **hLAIR-1: SmNPP5 Interaction was undetectable by SPR** – The hLAIR-1 analyte was injected across both Fc1 (Cd4 negative control control) and 2 (SmNPP5) between timepoints 5765 and 5825. A) Injection profile of Fc1 and Fc2. B) Subtracted Fc2-Fc1 curve. The hLAIR-1 analyte was injected at ~2μM.*

Indeed, both Fc 1 and 2 showed downward trends, which may reflect a change in buffer conditions upon injection of the analyte. No additional binding was observed in the flow cell containing the SmNPP5 protein compared to the flow cell containing the Cd4 negative control. This was attempted twice, giving the same result both times.

One of the main differences between the SAVEXIS and the SPR experiments is the composition of the buffer used: while the buffer used for SAVEXIS contains 2%BSA, the one used for SPR doesn't. This is noteworthy as BSA contains Zn^{2+} ions, and interestingly, SmNPP5 can coordinate three Zn2+ ions. So, we wanted to determine if the interaction between hLAIR-1 and SmNPP5 was dependant on the presence of the Zn2+ ion within SmNPP5 and supplied by the BSA, so we performed a SAVEXIS between SmNPP5 and hLAIR-1 in the presence of EDTA.

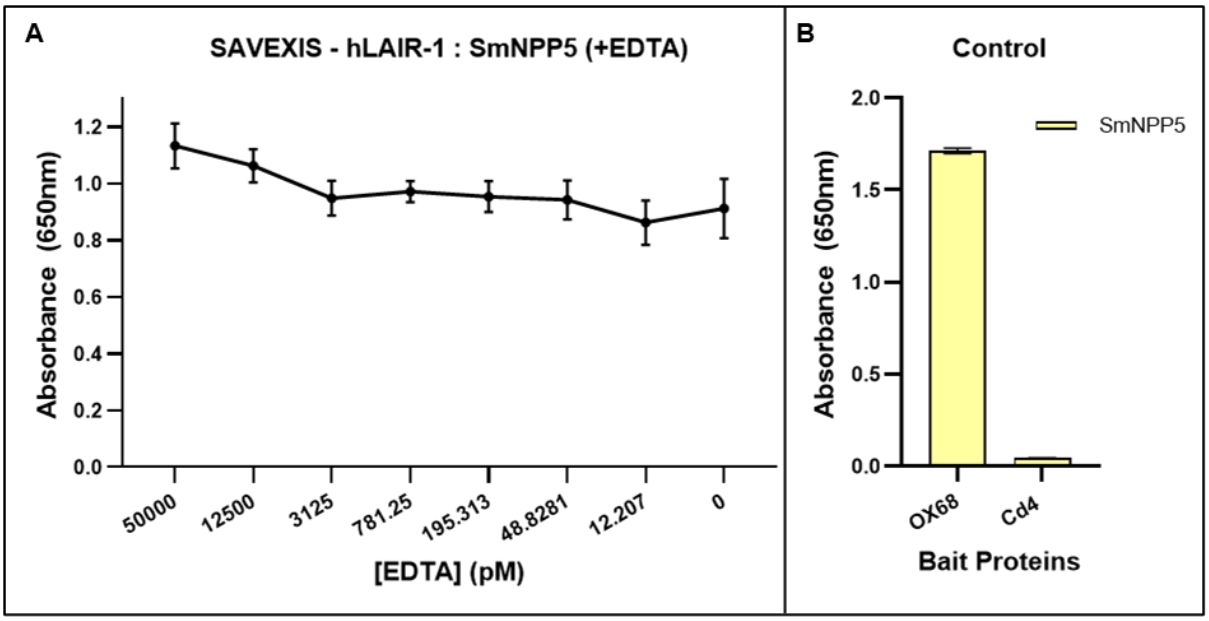

*Figure 14 - **EDTA does not affect SmNPP5 binding to hLAIR-1** – A) SAVEXIS between SmNPP5 and hLAIR-1 in the presence of different concentrations of EDTA with hLAIR-1 used as a bait and SmNPP5 used as a tetramerized prey. N=3. Error bars show +/- 1 standard deviation. B) OX68 bait is a positive control to show the prey is tetramerized. Cd4 bait is a negative control to show any background noise the prey may produce. N=3. Error bars show +/- 1 standard deviation.*

Figure 14 shows that EDTA had no effect on the hLAIR-1: SmNPP5 interaction across the range of concentrations tested. This experiment does have a caveat, as it was performed in HBS/ 2%BSA, which is the equivalent of 300μM BSA. BSA is known to bind Zn^{2+}, so the concentration of EDTA used in this experiment may not have been sufficient.

hLAIR-2 can also bind to SmNPP5

hLAIR-2 is a secreted paralog of hLAIR-1, so we hypothesised that it may also be a binding partner for SmNPP5. To test this, we included hLAIR-2 in a SAVEXIS against SmNPP5. hLAIR-2 is also known to bind to collagen at a higher affinity than hLAIR-1 (49), so we performed a new competition experiment with collagen to

determine if collagen could block any interaction found between hLAIR-2 and SmNPP5.

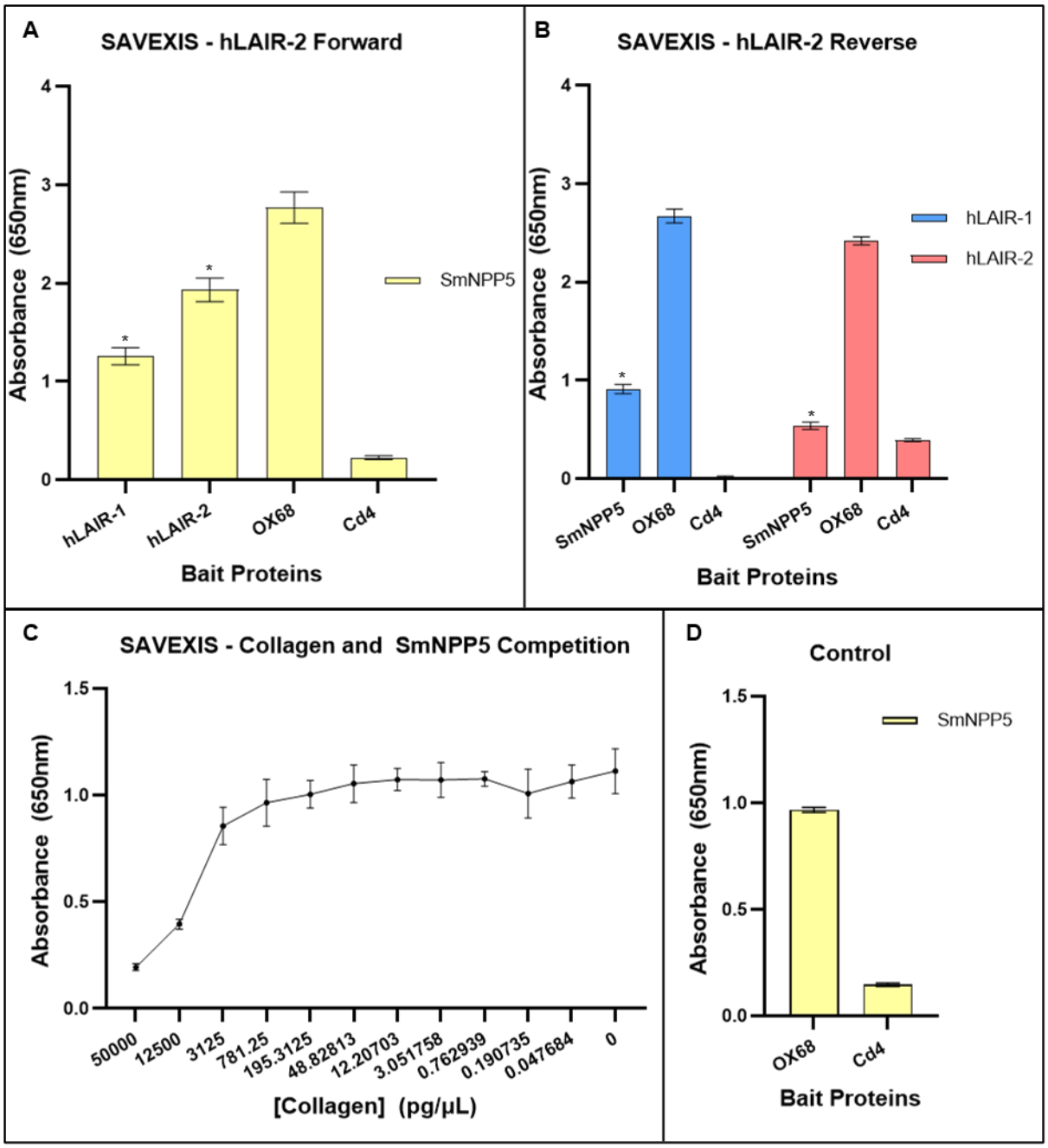

*Figure 15 - **hLAIR-2 can bind SmNPP5 –** A-B) SAVEXIS determination of binding of A) SmNPP5 prey tested against hLAIR-1 and hLAIR-2 baits. B) hLAIR-1 and hLAIR-2 prey interacting with the SmNPP5 bait. N=5. C) Shows a competition SAVEXIS between SmNPP5 and Collagen for hLAIR-2. hLAIR-2 was the bait, NPP5 was the tetramerized prey. N=3 D) Control for Panel C. The legend represents the prey protein used. OX68 is an antibody used as a positive control bait that specifically binds the Cd4 tag present on each recombinant protein. Cd4 is a negative control bait that should not bind prey, so revealing extent of non-specific interactions. Error bars represent mean -/+ standard deviation. Statistical significance determined by unpaired t-test compared to Cd4 negative control. (* represents p<0.0005).*

hLAIR-2 could bind to SmNPP5 irrespective of the bait: prey orientation (Fig. 15A, B). However, the hLAIR-2 prey gave a lot of background noise as observed with the Cd4 bait negative control (Fig. 15B). The hLAIR-2: SmNPP5 interaction could be blocked by concentrations of collagen I similar to the ones used to block the hLAIR1:SmNPP5 interaction. Therefore, hLAIR-2 behaves in a similar way to hLAIR-1 in regard to binding to SmNPP5.

4 – Discussion

In this study, we were able to replicate and reciprocate the SmNPP5 and hLAIR-1 interaction found in the initial screen via SAVEXIS and determined that the interaction is mediated by the Ig domain of hLAIR-1.

However, we had to show that our recombinant proteins were correctly folded and retained functionality. To provide this we used an anti-hLAIR-1 antibody, and a secondary verification of collagen I, as hLAIR-1 is a known collagen binding partner.

The dose-dependent binding of an anti-hLAIR-1 antibody to both the full-length and Ig domain of hLAIR-1 indicates the antibody-binding epitope is correctly folded. The disorganised region does not show this binding, dose-dependent or otherwise.

The binding of the full-length to collagen was expected, as collagen is the main binding partner for hLAIR-1 and acts as a positive control to compare the other results to. The binding of the Ig domain was also expected, as it contains the previously known key binding residues for collagen. With the binding of collagen present here, it provides evidence that both the full-length (Wildtype) and Ig domain of hLAIR-1 are correctly folded, because the collagen binding capacity is retained.

No binding function was observed for the disorganised region as the t-test value was not statistically significant from the negative control Cd4.

Overall, we show that the full length ectodomain and Ig domain bind to the full-length ectodomain of SmNPP5. We demonstrate that the binding is detectable in both orientations, which is not always the case with the SAVEXIS technique. With the hLAIR-1 Ig domain being the binding partner for SmNPP5, it is likely that all natural isoforms of hLAIR-1 can bind to SmNPP5, as the different isoforms have the same Ig domain, but different length of their disorganised regions (50).

Following this, we also aimed to gather evidence of SmNPP5 being correctly folded. To do so, we attempted to use a substrate that SmNPP5 is known to cleave, to show it had retained it enzymatic functionality. First, we used the substrate: p-nitrophenyl 5' TMP. This substrate has been previously used to demonstrate that SmNPP5 is catalytically active (42). However, when we attempted to use it, we found that the substrate was unstable at a pH above 4.5. This is unfortunate, as the optimal pH for SmNPP5 catalytic activity is at a pH of 9 (46). This meant that even if the catalytic activity was preserved in our recombinant SmNPP5, we could not detect it using this substrate.

One alternative option is to use ε-NAD (Nicotinamide 1,N6-ethenoadenine dinucleotide), a NAD analogue that contains a fluorophore within its structure. When turned over, the product is excited at 300 nm and emission occurs at 410 nm. We have started preliminary experiments, and we will attempt to measure substrate turnover in the future.

Despite this, we still went ahead with the SPR experiment, and during the setup for this, we had to use a gel filtration column to purify our proteins. When recombinant SmNPP5 was run on a gel filtration column, the elution profile suggested it could dimerise. Since this was surprising, we then used *in silico* predictions to determine if this was accurate. The AlphaFold multimer algorithm also predicted it could dimerise via a disulphide bridge.

Following this observation, it would be very informative to further characterize the impact that the dimerization of SmNPP5 has on the hLAIR-1: SmNPP5 interaction. While there are no other current reports that show SmNPP5 as a dimer, there are a few human NPP proteins that can form dimers: eNPP1 and eNPP3 (51). The role dimerization plays in the function of these enzymes has not currently been explored, but determining if the SmNPP5 dimerization is necessary for the interaction with hLAIR-1 would be a very informative experiment. To do this, we could mutate the cysteine responsible for the disulphide bridge (e.g. C410A), using site-directed mutagenesis and perform a SAVEXIS to determine if the monomeric form of SmNPP5 could still interact with hLAIR-1. Additionally, it would be informative to determine if the dimerization is necessary for the catalytic activity of SmNPP5. If we were able to determine catalytic activity using ε-NAD, we could use the C410A mutant mentioned earlier to determine if dimerization is required for catalytic activity by comparing it with the wildtype.

Moving on, we wanted to determine a potential binding site of SmNPP5, and to do this, we used AlphaFold to predict potential binding sites on SmNPP5. The most confident predictions suggested similar binding sites on the proteins. When we

attempted to mutated a binding residue, we found the N113A mutant was unable to express. However, mutating it to a different residue may allow it to express. We theorise this is because asparagine has an amide group at the end of its 2-carbon side chain, while alanine simply has a methyl group as its side chain (1-carbon). The highest confidence prediction predicts that the N113 residue binds to both S66 and T67 on hLAIR-1 using both hydrogens on the NH_2 of the amide group (Fig. 8). While it binds to S115 on itself, via a hydrogen bond using the C=O of the amide group. When we mutated this asparagine residue to an alanine, we removed the predicted binding to hLAIR-1 but we also removed predicted binding to itself. This may have caused the protein to unfold and may be the cause of an inability to express. Instead, we could mutate the asparagine to an aspartic acid (D) or potentially a serine (S). This would remove the NH_2 group that provides a hydrogen bond to hLAIR-1, while keeping either a C=O or OH in the same position as the asparagine did, still providing the hydrogen bond to itself. This may allow the protein to fold correctly and express, to then be tested for binding to hLAIR-1 via SAVEXIS.

Despite N113A not expressing, we have shown that the T108A SmNPP5 mutant is able to bind hLAIR-1, however it showed a diminished ability to bind compared to the wildtype. This suggests that the interaction requires T108 but is not entirely dependent upon it as it did not abolish the interaction completely.

Regardless, it would be extremely informative to create mutants of the other predicted binding residues and perform the exact same SAVEXIS to determine if they are involved in the interaction. Provided expression of said mutants was successful, this should help determine the binding residues of SmNPP5 in this interaction.

After this characterisation of the binding site, we showed the tetramerized prey SmNPP5 could compete with collagen I for the bait protein hLAIR-1. At a higher concentration of collagen I, the prey SmNPP5 was blocked from binding to the hLAIR-1 bait. However, at lower concentrations, the blocking of binding was absent, indicating the SmNPP5 prey outcompeted the collagen I for binding to hLAIR-1. It would also have been informative to see if SmNPP5 could block the collagen-hLAIR-1 interaction as well. Regardless, because we found that SmNPP5 competed with collagen for binding of hLAIR-1, we created hLAIR-1 mutants that may abolish binding to collagen to test if those same residues were responsible for binding to SmNPP5. The hLAIR-1 mutants R59A and R65A were chosen because they were previously shown to diminish collagen binding (48). Other mutants such as E61A were present in this previous study, which showed promise in reducing binding to collagen I too, and it would have been very informative to also use this residue in our study.

We tested these hLAIR-1 mutants' ability to bind to SmNPP5 in a SAVEXIS assay and showed that both hLAIR-1 residues R59 and R65 are critical for binding to SmNPP5. Interestingly, a paper studying RIFINs, which are proteins produced by *Plasmodium falciparum* (the parasite that causes malaria) were also found to bind hLAIR-1 (52). They showed that the RIFINs bind very similar residues on hLAIR-1 that collagen does, also suggesting that they compete for the same binding site.

To verify the lack of binding to collagen, we used these mutants in a SAVEXIS against collagen I. As expected, the R59A mutant was unable to bind to collagen, showing no statistically significant difference from the negative control. However, the R65A mutant was able to bind to collagen I. This could be explained by previous published observations (48) where R65A abolished binding to collagen III and IV, but

only diminished the binding to collagen I. As the SAVEXIS technique is designed to detect low-affinity interactions, it could still detect the interaction of the R65A hLAIR-1 to collagen I. Finally, we also demonstrated that SmNPP5 does not bind to collagen I. This is further evidence that collagen does not bridge the interaction between SmNPP5 and hLAIR1, and instead collagen I and SmNPP5 compete for the same (or similar) binding residues on hLAIR-1. These findings have now evolved our hypothesis. We theorize that SmNPP5 plays a role in downregulation of the immune system during the larval and worm stages of *Schistosoma mansoni and* does so by binding to hLAIR-1 at the same site collagen can, and may have the same effect collagen does when binding to hLAIR-1.

Because of these findings, we thought it critical to determine the binding affinity of the hLAIR-1 – SmNPP5 interaction. If it was a relatively strong interaction, then it would more evidence in support of our theory. The SPR experiment shown earlier was a preliminary experiment, and what was meant to proceed was the determination of binding affinity between SmNPP5 and hLAIR-1. However, the preliminary SPR experiment gave results that implied the interaction was not present at all. These results are puzzling as under normal conditions the analyte injection is seen as a large increase in response units in the ligand flow cell, while little change is observed in the reference flow cell. The lack of a spike in RUs at all is inconsistent with what is expected. This SPR experiment implies that hLAIR-1 and SmNPP5 do not interact, conflicting with our previous results. One theory we had was to do with the change in buffer for SPR (Not containing BSA). So the SAVEXIS with EDTA was done to test this theory. We found that the concentrations of EDTA tested had no effect on the interaction. In hindsight, we should have had a much higher

concentration of EDTA to bind the Zn^{2+} ions within the BSA mixture. It would not be possible to eliminate the BSA from the buffer as it is used as a blocking agent in the SAVEXIS, aiming to eliminate all non-specific binding from any contaminants that may enter the wells. So a much higher concentration of EDTA would be the best course of action here.

In our research for background knowledge surrounding hLAIR-1, we found a highly conserved relative to hLAIR-1: hLAIR-2. hLAIR-2 is a secreted protein that shares 85% of its conserved C2-like binding Ig domain with hLAIR-1, this includes many key residues such as R59, E61, R65, Y68, D70, W109 and E111. hLAIR-2 is an antagonist to hLAIR-1, it actually binds to collagen with a higher affinity (49) than hLAIR-1. Since hLAIR-2 displaces hLAIR-1 on collagen, it therefore decreases hLAIR1 activation, subsequently lowering hLAIR-1 activated immune modulation. Due to the high conservation of identity within the binding region, we decided to include hLAIR-2 in the project. We found that hLAIR2 could also bind SmNPP5 and the interaction be disrupted by addition of collagen I as an inhibitor. This is likely due to the high conservation of collagen binding residues between hLAIR-1 and 2, but equally it could indicate a more intricate system of immune regulation than we initially hypothesised:

Due to hLAIR-2 also being a tentative binding partner for SmNPP5, we propose an alternative theoretical mechanism for immunomodulation via SmNPP5: As SmNPP5 binds to hLAIR-2, it blocks hLAIR-2 from binding to collagen. That would allow hLAIR-1 to bind collagen and be activated, suppressing the immune response. Any excess SmNPP5 that does not bind hLAIR-2, could then bind hLAIR-1, bypassing

collagen and hLAIR-2 altogether and causing the same downstream effect. So regardless of if SmNPP5 binds hLAIR-1 or hLAIR-2, we propose that it has the same downstream effect. This theory of course relies on many assumptions that would need to be confirmed via experiments. It assumes that SmNPP5 binds to hLAIR-2 with the same or greater affinity as it does hLAIR-1. It assumes that the interaction happens in vivo. Finally, It assumes that the binding of SmNPP5 to hLAIR-1 activates hLAIR-1 in the same way collagen I does. If the theory were confirmed to be true, it would also be informative to know which interaction has a higher affinity, and subsequently, which interaction has the bigger downstream effect of immunomodulation. A good way to test this is with hLAIR-1 and hLAIR-2 knockout mice. This would be done by removing hLAIR-1 from the equation, and exclusively analysing what the downstream of the hLAIR-2 and SmNPP5 is. The alternative would also be done, removing hLAIR-2 but keeping hLAIR-1. By comparing the downstream effects of both these interactions separately *in* vivo, we could determine which interaction has the bigger downstream effect. Finally, it would be informative to know that if SmNPP5 binds hLAIR-2 with excess SmNPP5 bind hLAIR-1, if this causes a bigger downstream effect than binding either protein separately.

Future Directions

Because both hLAIR-1 and hLAIR-2 can bind to SmNPP5, it would be important to determine the binding affinity of both hLAIR-1 and hLAIR-2 to SmNPP5. Although the preliminary SPR experiment was not conclusive, we could have tried a variety of different buffer conditions or techniques to determine the binding affinity. However due to time constraints, this was not possible. Ideally, we would use multiple protein

batches, different buffers and a positive control. However, it may also be true that SPR is not the best method to determine the binding affinity for this interaction, instead, an alternative method like mass photometry could be used.

It would be very informative to mutate more residues on hLAIR-1 and test binding to SmNPP5, using the known collagen and RIFIN binding residues and predicted SmNPP5 binding residues as a guide. A non-exhaustive list is below (Table 2).

Collagen	RIFIN	SmNPP5
R59	R59	R59
E61	E61	R65
R65	R62	S66
T67	R65	T67
Y68	S66	Y68
N69	T67	D70
R100	Y68	W109
I102	N69	
W109	D70	
E111	W109	
Q112	E111	

*Table 2 – **Binding Residues for hLAIR-1 to Different Proteins.** Known binding residues are shown in black (52) and predicted binding residues in red. This is a non-exhaustive list, there are different types of collagens, each with slightly different binding residues on hLAIR-1. SmNPP5 predictions are from Figure 8.*

It would also be informative to test if binding of the RIFIN blocks binding of SmNPP5 to hLAIR-1, or vice versa. If both RIFIN and SmNPP5 bind for the same residues on hLAIR-1 then it may indicate that hLAIR-1 is a prevalent target of parasites within the human immune system. Determining the functional outcome of binding of these different parasite proteins may reveal an underlying mechanism in parasite immunoregulation.

To determine if SmNPP5 can bind to hLAIR-1 in vivo, we could use flow cytometry to observe if recombinant SmNPP5 can bind to hLAIR-1 expressing cells. It may also be worth testing other tegumental ecto-enzymes in a similar way, such as SmATPase1 and SmAP (19,20). However, with hLAIR-2 being a secreted protein, a different approach would have to be used. Instead, we could use recombinant hLAIR-2 to detect binding to the worm tegument directly. This would not confirm that it is only binding to SmNPP5, but it would confirm it binds *in vivo*.

To study the functional effects of any detected binding in vivo, and in particular whether binding of SmNPP5 can trigger hLAIR1 activation and play a role in the regulation of the immune system, different cellular read-outs could be used. As hLAIR-1 is found on a variety of leukocytes, and the downstream effects of hLAIR-1 activation on these leukocytes has already been well characterized, there are many to choose from. For example, hLAIR-1 activation on B-cells leads to the decrease of IgG and IgE secretion (36). In addition, activation of hLAIR1 can be monitored in NFAT:GFP cells (28) or through the use of anti-phospho-SHP1 antibodies to monitor activation of the signalling cascade downstream of hLAIR1. Observing if SmNPP5 can cause such downstream effects would be very informative. Additionally, functional experiments for SmNPP5 would also be very informative. One example would be using RNAi interference on SmNPP5, or SmNPP5-knockdown schistosomula and co-culturing them with immune cells to measure the cytokine production when SmNPP5 is present or absent. We know RNAi of SmNPP5 has already been used to determine that SmNPP5 is a virulence factor for *S. mansoni* (42), so this established method could be used to further our current hypothesis. This experiment could reveal some other immunoregulatory interactions caused by

SmNPP5 that may not have been detected by the initial SAVEXIS screen. It would also be another way of testing whether the SmNPP5 - hLAIR-1 interaction actually occurs *in vivo*. Finally, to further characterize the binding site of this interaction, X-ray crystallography would be a definitive way to confirm the binding residues of both SmNPP5 and hLAIR-1, the reason it was not done here, was due to the previously mentioned time constraints.

Summary of Conclusions

We have found that the domain of hLAIR-1 binding to SmNPP5 is the Ig domain. Two specific residues hLAIR-1 used to bind to SmNPP5 are R59 and R65, however we were unable to identify essential binding residues for SmNPP5. We have determined that SmNPP5 is a natural dimer and is likely bridged through a disulphide bond between C410. We have also found that SmNPP5 and collagen I compete for the same binding site on hLAIR-1, and an excess of collagen I can block binding of SmNPP5. Finally, we have found that SmNPP5 can bind the hLAIR-1 antagonist, hLAIR-2, and that SmNPP5 will compete with collagen I for hLAIR-2 as well. Given the wide distribution of expression of the immunosuppressive receptor hLAIR1 on the surface of host immune cells, and the persistent expression of SmNPP5 on the surface of the parasite, it is conceivable that the interaction between these two proteins would have a significant role in immune regulation. Future experiments will shed light on whether SmNPP5 can activate LAIR1 to promote parasite survival in the infected host

References

1. P Steinmann, J Keiser, R Bos, M Tanner, J Utzinger. Schistosomiasis and water resources development: systematic review, meta-analysis, and estimates of people at risk. The Lancet Infectious Diseases. 2006; 6(7): 411-425.

2. World Health Organization. Schistosomiasis and soil transmitted helminthiases: number of people treated in 2016. Weekly Epidemiological Report. 2017; 8: 249-260.

3. D G Colley, A L Bustinbuy, W E Secor, C H king. Human schistosomiasis. The Lancet. 2014; 383(9936): 2253-2234.

4. C Huot, C Clerissi, B Gourbal, R Galinier, D Duval and E Toulza. Schistosomiasis Vector Snails and Their Microbiota Display a Phylosymbiosis Pattern. Frontiers in Microbiology. 2020; PMID: 32082267

5. J D Lawrence. The Ingestion of Red Blood Cells by Schistosoma mansoni. The Journal of Parasitology. 1973 Feb; 59(1): 60-63.

6. K Peterková, L Konečný, T Macháček, L Jedličková, F Winkelmann, M Sombetzki et al. Winners vs. losers: Schistosoma mansoni intestinal and liver eggs exhibit striking differences in gene expression and immunogenicity. PLOS Pathogens. 2024 May; 20(5): e1012268.

7. M S Wilson, M M Mentink-Kane, J T Pesce, T R Ramalingam, R Thompson and T A Wynn. Immunopathology of schistosomiasis. Immunology and Cell Biology. 2006, 85(2): 148-154.

8. BioRender. Created with Biorender.com. 2024

9. L Richards, B Erko, K Ponpetch, S J Ryan and S Liang. Assessing the nonhuman primate reservoir of Schistosoma mansoni in Africa: a systematic review. Infectious Diseases of Poverty. 2019 May; 8: Article 32

10. S Catalano, M Sène, N D Diouf, C B Fall, A Borlase, E Léger et al. Rodents as Natural Hosts of Zoonotic Schistosoma Species and Hybrids: An Epidemiological and Evolutionary Perspective From West Africa. The Journal of Infectious Diseases. 2018 Aug; 218(3): 429–433

11. CDC. Center for Disease Control and Prevention. [Online].; 2019 [cited 2024 01 26. Available from: https://www.cdc.gov/dpdx/schistosomiasis/index.html.

12. M L Burke, M K Jones, G N Gobert, Y S Li, M K Ellis, D P McManus. Immunopathogenesis of human schistosomiasis. Parasite Immunology. 2009; 31(4): 163-176.

13. M J Doenhoff, D Cioli, J Utzinger. Praziquantel: mechanisms of action, resistance and new derivatives for schistosomiasis. Current Opinion in Infectious Diseases. 2008; 21(6): 659-667.

14. W Le Clec'h, F D Chevalier, A C A Mattos, A Strickland, R Diaz, M McDew-White et al. Genetic analysis of praziquantel response in schistosome parasites implicates a Transient Receptor Potential channel. Science Translational Medicine. 2021 December; 13(625).

15. A Danso-Appiah, S J De Vlas. Interpreting low praziquantel cure rates of Schistosoma mansoni infections in Senegal. Trends in Parasitology. 2002; 18(3): 125-129.

16. M J Doenhoff, J R. Kusel, G C Coles, D Cioli. Resistance of Schistosoma mansoni to praziquantel: is there a problem? Transactions of The Royal Society of Tropical Medicine and Hygiene. 2002; 96(5): 465-469.

17. P J Brindley, A Sher. The chemotherapeutic effect of praziquantel against Schistosoma mansoni is dependent on host antibody response. Journal of immunology. 1987; 139(1): 215–220.

18. A H Costain, A T Phythian-Adams, S A P Colombo, A K Marley, C Owusu, P C Cook et al. Dynamics of host immune response development during Schistosoma mansoni infection. Frontiers in Immunology. 2022 Jul; 13: 906338.

19. A A Da'dara, R Bhardwaj, Y B M Ali, P J Skelly. Schistosome tegumental ecto-apyrase (SmATPDase1) degrades exogenous pro-inflammatory and pro-thrombotic nucleotides. PeerJ. 2014 Mar; 2: e316

20. S Acharya, A A Da'dara and P J Skelly. Schistosome immunomodulators. PLoS Pathog. 2021 Dec; 17(12): e1010064

21. K Knuhr, K Langhans, S Nyenhuis, K Viertmann, A M Overgaard Kildemoes, M J Doenhoff et al. Schistosoma mansoni Egg-Released IPSE/alpha-1 Dampens Inflammatory Cytokine Responses via Basophil Interleukin (IL)-4 and IL-13. Frontiers in Immunology. 2018 Oct; 9

22. P J Skelly, A A Da'dara. Schistosome secretomes. Acta Tropica. 2022 Oct; 236: 106676.

23. J Shilts, Y Severin, F Galaway, N Müller-Sienerth, Z-S Chong, S Pritchard et al. A physical wiring diagram for the human immune system. Nature. 2022; 608: 397-404.

24. C Crosnier, C H Hokke, A V Protasio, C Brandt, G Rinaldi, M C C Langenberg et al. Screening of a Library of Recombinant Schistosoma mansoni Proteins With Sera From Murine and Human Controlled Infections Identifies Early Serological Markers. The Journal of Infectious Diseases. 2020 Jun; 225(8): 1435–1446.

25. N Guo, K Zhang, X Gao, M Lv, J Luan, Z Hu et al. Role and mechanism of LAIR-1 in the development of autoimmune diseases, tumors, and malaria: A review. Current Research in Translational Medicine. 2020 Jun; 68(3): 119–124

26. F V Laethem, L Donaty, E Tchernonog, V Lacheretz-Szablewski, J Russello, D Buthiau et al. LAIR1, an ITIM-Containing Receptor Involved in Immune Disorders and in Hematological Neoplasms. International Journal of Molecular Sciences. 2022; 23(24): 16136.

27. A Verbrugge, T de Ruiter, H Clevers, L Meyaard. Differential contribution of the immunoreceptor tyrosine-based inhibitory motifs of human leukocyte-associated Ig-like receptor-1 to inhibitory function and phosphatase recruitment. International immunology. 2003; 15(11): 1349-1358.

28. R J Lebbink, T de Ruiter, J Adelmeijer, A B Brenkman, J M van Helvoort, M Koch et al. Collagens are functional, high affinity ligands for the inhibitory immune receptor LAIR-1. Journal of Experimental Medicine. 2006; 203(6): 1419-1425.

29. S Kim, E R Easterling, L C Price, S L Smith, J E Coligan, J-E Park et al. The Role of Leukocyte Associated Immunoglobulin-Like Receptor-1 (LAIR-1) in Suppressing Collagen-Induced Arthritis. J Immunol. 2017 Sep 8;199(8):2692–2700.

30. M Son, F Santiago-Schwarz, Y Al-Abed, B Diamond. C1q limits dendritic cell differentiation and activation by engaging LAIR-1. Proceedings of the National Academy of Sciences of the United States of America. 2012; 109(46): E3160–E3167

31. M J M Olde Nordkamp, M van Eijk, R T Urbanus, L Bont, P Haagsman, L Meyaard, Leukocyte-associated Ig-like receptor-1 is a novel inhibitory receptor for surfactant protein D. Journal of Leukocyte Biology. 2014; 96(1): 105-111.

32. J Jumper, R Evans, A Pritzel, T Green, M Figurnov, O Ronneberger et al. Highly accurate protein structure prediction with AlphaFold. Nature. 2021; 596: 583-589.

33. M Varadi, S Anyango, M Deshpande, S Nair, C Natassia, G Yordanova et al. AlphaFold Protein Structure Database: massively expanding the structural coverage of protein-sequence space with high-accuracy models. Nucleic Acids Research. 2022; 50(D1): D439–D444.

34. A O Achieng, B Guyah, Q Cheng, J M Ong'echa, C Ouma, C G Lambert et al. Molecular basis of reduced LAIR1 expression in childhood severe malarial anaemia: Implications for leukocyte inhibitory signalling. EBioMedicine. 2019 Jul; 45: 278-289

35. L Meyaard, G J Adema, C Chang, E Woollatt, G R Sutherland, L L Lanier et al. LAIR-1, a novel inhibitory receptor expressed on human mononuclear leukocytes. Immunity. 1997; 7(2): 283-290.

36. A R van der Vuurst de Vries, H Clevers, T Logtenberg, L Meyaard. Leukocyte-associated immunoglobulin-like receptor-1 (LAIR-1) is differentially expressed during human B cell differentiation and inhibits B cell receptor-mediated signaling. European Journal of Immunology. 1999; 29(10): 3160–3167.

37. L Meyaard, J Hurenkamp, H Clevers, L L Lanier, J H Phillips. Leukocyte-associated Ig-like receptor-1 functions as an inhibitory receptor on cytotoxic T cells. Journal of Immunology. 1999; 162(10): 5800–5804.

38. T Carvalheiro, S Garcia, M I P Ramos, B Giovannone, T R D J Radstake, W Marut, et al. Leukocyte Associated Immunoglobulin Like Receptor 1 Regulation and Function on Monocytes and Dendritic Cells During Inflammation. Frontiers in Immunology. 2020; 11: 1793.

39. A Poggi, E Tomasello, E Ferrero, M R Zocchi, L Moretta. p40/LAIR-1 regulates the differentiation of peripheral blood precursors to dendritic cells induced by granulocyte-monocyte colony-stimulating factor. European Journal of Immunology. 1998; 28(7): 2086–2091.

40. I Bonaccorsi, C Cantoni, P Carrega, D Oliveri, G Lui, R Conte et al. The immune inhibitory receptor LAIR-1 is highly expressed by plasmacytoid dendritic cells and acts complementary with NKp44 to control IFNα production. Public Library of Science. 2010; 5(11): e15080

41. C L D Soria, J Lee, T Chong, A Coghlan, A Tracey, M D Young et al. Single-cell atlas of the first intra-mammalian developmental stage of the human parasite Schistosoma mansoni. Nature Communications. 2020; 11(6411).

42. R Bhardwaj, G Krautz-Peterson, A Da'dara, S Tzipori, and P J Skelly. Tegumental Phosphodiesterase SmNPP-5 Is a Virulence Factor for Schistosomes. Infection and immunity. 2011; 79(10): 4276-4284.

43. J J van Hellemond, K Retra, J F H M Brouwers, B W M van Balkom, M Yazdanbakhsh, C B Shoemaker et al. Functions of the tegument of schistosomes: clues from the proteome and lipidome. International Journal for Parasitology. 2006; 36(6): 691-699.

44. M Dagenais, L Tritten. Hidden in plain sight: How helminths manage to thrive in host blood. Frontiers in Parasitology. 2023; 2.

45. C S Nation, A A Da'Dara, P J Skelly. The essential schistosome tegumental ectoenzyme SmNPP5 can block NAD-induced T cell apoptosis. Virulence. 2020; 11(1): 568-579.

46. M Elzoheiry, A A Da'dara, A M deLaforcade, S N El-Beshbishi and P J Skelly. The Essential Ectoenzyme SmNPP5 from the Human Intravascular Parasite Schistosoma mansoni is an ADPase and a Potent Inhibitor of Platelet Aggregation. Thrombosis and Haemostasis. 2018 Jun; 118(6): 979-989.

47. R Borza, F Salgado-Polo, W H Moolenaar and A Perrakis. Structure and function of the ecto-nucleotide pyrophosphatase/phosphodiesterase (ENPP) family: Tidying up diversity. The Journal of biological chemistry. 2022 Dec; 298(2): 101526.

48. T Harma C Brondijk, T de Ruiter, J Ballering, H Wienk, R J Lebbink, H van Ingen et al. Crystal structure and collagen-binding site of immune inhibitory receptor LAIR-1: unexpected implications for collagen binding by platelet receptor GPVI. Blood. 2010 Feb; 115(7): 1364–1373.

49. M I P Ramos, L Tian, E J de Ruiter, C Song, A Paucarmayta, A Singh et al. Cancer immunotherapy by NC410, a LAIR-2 Fc protein blocking human LAIR-collagen interaction. eLife. 2021 Jun; 10: e62927.

50. L Meyaard. The inhibitory collagen receptor LAIR-1 (CD305). Journal of Leukocyte Biology. 2008 Apr; 83(4): 799–803.

51. R Borza, F Salgado-Polo, W H Moolenaar, A Perrakis. Structure and function of the ecto-nucleotide pyrophosphatase/phosphodiesterase (ENPP) family: Tidying up diversity. Journey of Biological Chemistry. 2021 Dec; 298(2): 101526.

52. Y Xie, X Li, Y Chai, H Song, J Qi and G F Gao. Structural basis of malarial parasite RIFIN-mediated immune escape against LAIR1. Cell reports. 2021 Aug; 36(8): 109600.

Appendix

1 - Primer List

LAIR-1 Ig Domain Forward – GCGGCCGCCACCATGGCTCCAC
LAIR-1 Ig Domain Reverse – GGCGCGCCGCTTGTTTCCTTCACCAGCAGC
LAIR-1 Disorganised Forward – ATGCGGCCGCCGGTGGACCTGACAGTCCCGAC
LAIR-1 Disorganised Reverse – GGCGCGCCGCTTGTTTCCTTCACCAGCAGC
NPP5 N-Terminus Forward – GCGGCCGCCTCTGGCGTCGTGGGCAAAGAA
NPP5 N-Terminus Reverse – GGCGCGCCGCTGATGTTGGTCATGCCGTGG
NPP5 C-Terminus Forward – GCGGCCGCCAGCGACAGAGTGATCTACCTG
NPP5 C-Terminus Reverse – GGCGCGCCAGACAGTCTGTTGATATTGGCG
LAIR-1 R59A Forward – GGTGTGCAGACTTTT**GCA**CTGGAAAGGGAGAGTC
LAIR-1 R59A Reverse – GACTCTCCCTTTCCAG**TGC**AAAAGTCTGCACACC
LAIR-1 R65A Forward – CTGGAAAGGGAGAGT**GCC**TCCACATACAACGATAC
LAIR-1 R65A Reverse – GTATCGTTGTATGTGGA**GGC**ACTCTCCCTTTCCAG
NPP5 T108A Forward - CCCATCATCAACGCC**GCC**TTCAGCAGCCGGAAC
NPP5 T108A Reverse - GTTCCGGCTGCTGAA**GGC**GGCGTTGATGATGGG
NPP5 N113A Forward - ACCTTCAGCAGCCGG**GCC**CAGAGCACCGCCACC
NPP5 N113A Reverse – GGTGGCGGTGCTCTG**GGC**CCGGCTGCTGAAGGT

497 – TGAGATCCAGCTGTTGGGGT
4006 – GGCGCGCCGCTTGTTTCCTTCACCAGCAGC

Mutated Bases in Red

2 – Buffers

Luria Bertani Broth: 1% Tryptone, 0.5% Yeast Extract, 171μM NaCl.

All following buffers were vacuum filtered through 0.22μm filter

Binding Buffer: 30mM Imidazole, 500mM NaCl, 3.8mM NaH_2PO_4, 16.2mM Na_2HPO_4, pH=7.4.

Elution Buffer: 400mM Imidazole, 500mM NaCl, 3.8mM NaH_2PO_4, 16.2mM Na_2HPO_4, pH=7.4.

HEPES Buffer Saline (HBS) 10X: 1.4M NaCl, 49.6mM KCl, 19.7mM $CaCl_2 \cdot 2H_2O$, 9.8nM $MgCl_2 \cdot 6H_2O$, 99.9mM HEPES, pH = 7.4.

HBS/T: 1X HBS, 0.1% TWEEN-20.

HBS/T desthiobiotin: 1X HBS, 0.1% TWEEN-20, 0.793nM desthiobiotin.

HBS/ 2% BSA: 1X HBS, 2% Bovine Serum Albumin (BSA).

Surface Plasmon Resonance (SPR) Buffer: 1X HBS, 60mM NaCl, 0.05% TWEEN-20.

Phosphate Buffer Saline 10X: 1.3689M NaCl, 26.8273mM KCl, 101.437mM Na_2HPO_4, 14.6966mM KH_2PO_4, pH = 7.4.

P-nitrophenyl 5' dTMP Buffer: 50 mM Tris-HCl buffer [pH 8.9], 120 mM NaCl, 5.0 mM KCl, 60 mM glucose, 0.5 mM phosphodiesterase chromogenic substrate p-nitrophenyl 5′-dTMP (p-Nph-5′-TMP) (Sigma-Aldrich).

ε-NAD Buffer: 50 mM Tris-HCl buffer [pH 8.9], 120 mM NaCl, 5.0 mM KCl, 60 mM glucose, 2mM $CaCl_2$. 0.5μM of ε-NAD (Sigma-Aldrich).

Tris Acetate EDTA (**TAE):** 1.9977M Tris base, 0.0571% Glacial Acetic acid, 63.6455mM EDTA.